Pressure- and Work-Limited Neuroadaptive Control for Mechanical Ventilation of Critical Care Patients

Konstantin Y. Volyanskyy, *Member, IEEE*, Wassim M. Haddad, *Fellow, IEEE*, and James M. Bailey

Abstract—**In this paper, we develop a neuroadaptive control architecture to control lung volume and minute ventilation with input pressure constraints that also accounts for spontaneous breathing by the patient. Specifically, we develop a pressure- and work-limited neuroadaptive controller for mechanical ventilation based on a nonlinear multicompartmental lung model. The control framework does not rely on any averaged data and is designed to automatically adjust the input pressure to the patient's physiological characteristics capturing lung resistance and compliance modeling uncertainty. Moreover, the controller accounts for input pressure constraints as well as work of breathing constraints. Finally, the effect of spontaneous breathing is incorporated within the lung model and the control framework.**

Index Terms—**Compartmental systems, mechanical ventilation, multicompartment lung model, neuroadaptive control, pressure-limited ventilation, work-limited ventilation.**

I. Introduction

The lungs are particularly vulnerable to acute critical illness. Respiratory failure can result not only from primary lung pathology, such as pneumonia, but also as a secondary consequence of heart failure or inflammatory illness, such as sepsis or trauma. When this occurs, it is essential to support patients while the fundamental disease process is addressed. For example, a patient with pneumonia may require mechanical ventilation while the pneumonia is being treated with antibiotics, which will eventually effectively "cure" the disease. Since the lungs are vulnerable to critical illness and respiratory failure is common, support of patients with mechanical ventilation is very common in the intensive care unit.

The goal of mechanical ventilation is to ensure adequate ventilation, which involves a magnitude of gas exchange that leads to the desired blood level of carbon dioxide (CO_2), and adequate oxygenation, which involves a blood concentration of oxygen that will ensure organ function. Achieving these goals is complicated by the fact that mechanical ventilation can actually cause acute lung injury, either by inflating the lungs to excessive volumes or by using excessive pressures to inflate the lungs. The challenge to mechanical ventilation is to produce the desired blood levels of CO_2 and oxygen without causing further acute lung injury.

The earliest primary modes of ventilation can be classified, approximately, as volume-controlled or pressure-controlled [1]. In volume-controlled ventilation, the lungs are inflated (by the mechanical ventilator) to a specified volume and then allowed to passively deflate to the baseline volume. The mechanical ventilator controls the volume of each breath and the number of breaths per minute. In pressure-controlled ventilation, the lungs are inflated to a given peak pressure. The ventilator controls this peak pressure as well as the number of breaths per minute. In early ventilation technology, *negative pressure ventilation* was employed, wherein a patient's thoracic area is enclosed in an airtight chamber and the volume of the chamber is expanded, inflating the patient's lungs. Such ventilator devices include tank ventilators, jacket ventilators, and cuirassess [2].

The primary determinant of the level of CO_2 in the blood is *minute ventilation*, which is defined as the *tidal volume* (the volume of each breath) multiplied by the number of breaths per minute [3], [4]. With volume-controlled ventilation, both tidal volume and the number of breaths are determined by the machine (the ventilator), and typically, the tidal volumes and breaths per minute are selected by the clinician caring for the patient. In pressure-controlled ventilation, the tidal volume is not directly controlled. The ventilator determines the pressure that inflates the lungs and the tidal volume is proportional to this driving pressure and the compliance or "stiffness," of the lungs. Consequently, the minute ventilation is not directly controlled by the ventilator and any change in lung compliance (such as improvement or deterioration in the underlying lung pathology) can result in changes in tidal volume, minute ventilation, and ultimately, the blood concentration of CO_2.

In respiratory management, the goal is to control arterial partial pressure of CO_2 in the blood denoted by $P_{\mathrm{a}}CO_2(t)$. The means to do this is reflected in the equation relating $P_{\mathrm{a}}CO_2(t)$ to the volume of gas exchange in the lungs in a given unit of time, the *alveolar ventilation*. The relationship between $P_{\mathrm{a}}CO_2(t)$ and ventilation is given by [3]

$$P_{\mathrm{a}}CO_2(t) = 0.863\frac{VCO_2}{V_{\mathrm{a}}(t)}, \qquad t \geq 0$$

where VCO_2 is the total body production of CO_2 per minute, which is approximately 259 $\mathrm{m}\ell$/min in healthy subjects, 0.863 is a constant to reconcile units, and $V_{\mathrm{a}}(t)$ is alveolar venti-

Manuscript received February 14, 2010; revised October 13, 2010 and January 20, 2011; accepted January 23, 2011. Date of publication March 14, 2011; date of current version April 6, 2011. This work was supported in part by the U.S. Army Medical Research and Material Command, under Grant 08108002.

K. Y. Volyanskyy and W. M. Haddad are with the School of Aerospace Engineering, Georgia Institute of Technology, Atlanta, GA 30332 USA (e-mail: gtg891s@mail.gatech.edu; wm.haddad@aerospace.gatech.edu).

J. M. Bailey is with the Department of Anesthesiology, Northeast Georgia Medical Center, Gainesville, GA 30503 USA (e-mail: james.bailey@nghs.com).

Digital Object Identifier 10.1109/TNN.2011.2109963

lation. In patients who are totally dependent on mechanical ventilation (and not taking any independent breaths), $V_a(t)$ is given by [3]

$$V_a(t) = (TV(t) - V_d)RR(t), \qquad t \geq 0$$

where $TV(t)$ denotes the volume of each breath set on the ventilator (i.e., tidal volume), $RR(t)$ denotes the respiratory rate set on the ventilator, and V_d denotes the dead space of the lungs. The product $TV(t)RR(t)$ is referred to as *minute ventilation* [3] and V_d is approximately one-third of minute ventilation in healthy subjects. During mechanical ventilation $TV(t) \in [400, 700]$ mℓ and $RR(t) \in [12, 25]$. The tidal volume is the difference between the lung volume at the start of expiration and the lung volume at the end of expiration.

In this paper, we will denote the lung volume by $V(t)$ and the inspiration time and expiration time by T_{in} and T_{ex}, respectively, over a single breathing cycle $T = T_{in} + T_{ex}$. Furthermore, we assume that the inspiration process starts from a given initial state $V(0)$ and is followed by the expiration process where its initial state is the final state of inspiration. Hence, the explicit relationship between the delivered air volume and the tidal volume over a ventilatory cycle is given by $TV = V(T_{in}) - V(T_{in} + T_{ex}) = V(T_{in}) - V(0)$.

The concentration of oxygen in the blood is determined by the underlying lung pathology, the concentration of oxygen in the gas delivered by the mechanical ventilator, and also by the pressure that is used to inflate the lungs. In very general terms, oxygenation can be improved by higher mean pressures in the lungs, although higher peak pressures during the inflation–deflation cycle are associated with lung injury [5], [6].

With the increasing availability of microchip technology, it has been possible to design mechanical ventilators that have control algorithms which are more sophisticated than simple volume or pressure control. Examples are proportional-assist ventilation [7], [8], adaptive support ventilation [9], SmartCare ventilation [10], and neurally adjusted ventilation [11]. In proportional-assist ventilation, the ventilator measures the patient's volume and rate of inspiratory gas flow, and then applies pressure support in proportion to the patient's inspiratory effort [12]. In this mode of ventilation, inspired oxygen and positive end-expiratory pressure are manually adjusted by the clinician.

In adaptive support ventilation, tidal volume and respiratory rate are automatically adjusted [13]. In particular, minute ventilation $(TV(t)RR(t))$ is calculated from a % MinVol parameter and the patient's ideal body weight. The patient's respiratory pattern is measured pointwise in time and fed back to the controller to provide the required (target) tidal volume and patient respiratory rate. Adaptive support ventilation does not provide continuous control of minute ventilation, positive end-expiratory pressure, and inspired oxygen, these parameters need to be adjusted manually.

SmartCare ventilation monitors tidal volume, respiratory rate, and end-tidal pressure of CO_2 to maintain the patient in a respiratory "comfort" zone by automatically adjusting the level of pressure support [14], [15]. SmartCare ventilators do not account for patient respiratory variations and do not generally guarantee adequate minute ventilation during weaning. In addition, positive end-expiratory pressure and inspired oxygen need to be manually adjusted.

Neurally adjusted ventilation is fundamentally different from the aforementioned automatic ventilation technologies in the sense that it uses the patient's respiratory neural drive as a measurement signal to the ventilator [16]. In this mode of ventilation, rather than controlling pressure, the patient's respiratory neural drive signal to the diaphragmatic electromyogram is controlled using electrodes placed on an esophageal catheter [17]. Even though this approach has been shown to be effective in some recent clinical studies [18], [19], its effectiveness is affected if the patient is highly sedated. In addition, as in the aforementioned ventilator technologies, positive end-expiratory pressure and inspired oxygen need to be manually controlled.

The common theme in modern ventilation control algorithms is the use of pressure-limited ventilation while also guaranteeing adequate minute ventilation. One of the challenges in the design of efficient control algorithms is that the fundamental physiological variables defining lung function, i.e., the resistance to gas flow and the compliance of the lung units, are not constant but rather vary with lung volume. This is particularly true for compliance, strictly defined as $\mathrm{d}V/\mathrm{d}P$, where V is the lung unit volume and P is the pressure driving inflation. More simply, lung volume is a nonlinear function of driving pressure. In addition, these physiological variables vary from patient to patient, as well as within the same patient under different conditions, making it very challenging to develop models and effective control law architectures for active mechanical ventilation.

In this paper, we develop an adaptive control architecture to control lung volume and minute ventilation with input pressure constraints that also accounts for spontaneous work of breathing by the patient. Specifically, we develop a pressure- and work-limited neuroadaptive controller for mechanical ventilation based on a nonlinear multicompartmental lung model. The control framework does not rely on any averaged data and is designed to automatically adjust the input pressure to the patient's physiological characteristics, capturing lung resistance and compliance modeling uncertainty. Moreover, the controller accounts for input pressure constraints as well as work of breathing constraints. Finally, the effect of spontaneous breathing is incorporated within the lung model and the control framework.

The contents of this paper are as follows. In Section II, we provide definitions and mathematical preliminaries on nonlinear nonnegative dynamical systems that are necessary for developing the main results of this paper. In Section III, we develop a neuroadaptive control framework for nonnegative dynamical systems with actuator amplitude and control integral constraints. It is important to note here that, even though adaptive and neuroadaptive controllers for nonnegative dynamical systems have been developed in the literature [20]–[24], neuroadaptive control with actuator saturation and integral constraints is virtually nonexistent. Notable exceptions include [25] (see also [26]). Then, in Section IV, we extend the linear multicompartment lung model given in [27] to address system model nonlinearities and spontaneous patient work of breathing effects. To demonstrate the efficacy of the proposed neuroadaptive control framework, in Section V we apply our framework to control the ventilatory drive of a pressure- and work-limited respirator in the face of lung modeling uncertainty. Finally, in Section VI we draw conclusions.

II. Mathematical Preliminaries

In this section, we introduce notation, several definitions, and some key results concerning nonlinear nonnegative dynamical systems [28], [29] that are necessary for developing the main results of this paper. Specifically, for $x \in \mathbb{R}^n$ we write $x \geq\geq 0$ (resp., $x >> 0$) to indicate that every component of x is nonnegative (resp., positive). In this case, we say that x is *nonnegative* or *positive*, respectively. Likewise, $A \in \mathbb{R}^{n\times m}$ is *nonnegative*[1] or *positive* if every entry of A is nonnegative or positive, respectively, which is written as $A \geq\geq 0$ or $A >> 0$, respectively. Furthermore, let $\overline{\mathbb{R}}_+^n$ and $\mathbb{R}_+^n$ denote the nonnegative and positive orthants of $\mathbb{R}^n$: that is, if $x \in \mathbb{R}^n$, then $x \in \overline{\mathbb{R}}_+^n$ and $x \in \mathbb{R}_+^n$ are equivalent, respectively, to $x \geq\geq 0$ and $x >> 0$. Finally, we write $(\cdot)^{\mathrm{T}}$ to denote transpose, $(\cdot)'$ to denote Fréchet derivative, $\operatorname{tr}(\cdot)$ for the trace operator, $\lambda_{\min}(\cdot)$ (resp., $\lambda_{\max}(\cdot)$) to denote the minimum (resp., maximum) eigenvalue of a Hermitian matrix, and $\|\cdot\|$ for a vector norm in $\mathbb{R}^n$.

Definition 1: Let $T > 0$. A real function $u : [0, T] \to \mathbb{R}^m$ is a *nonnegative* (resp., *positive*) *function* if $u(t) \geq\geq 0$ (resp., $u(t) >> 0$) on the interval $[0, T]$.

The following definition introduces the notion of essentially nonnegative vector fields [28], [29].

Definition 2: Let $f = [f_1, \ldots, f_n]^{\mathrm{T}} : \mathcal{D} \subseteq \overline{\mathbb{R}}_+^n \to \mathbb{R}^n$. Then f is *essentially nonnegative* if $f_i(x) \geq 0$ for all $i = 1, \ldots, n$ and $x \in \overline{\mathbb{R}}_+^n$ such that $x_i = 0$, $i = 1, \ldots, n$, where x_i denotes the ith component of x.

It follows from Definition 2 that, if x_i is an element of the boundary of $\overline{\mathbb{R}}_+^n$, then $f_i(\cdot)$ is directed toward $\overline{\mathbb{R}}_+^n$. In addition, note that, if $f(x) = Ax$, where $A \in \mathbb{R}^{n\times n}$, then f is essentially nonnegative if and only if A is *essentially nonnegative* or *Metzler*: that is, $A_{(i,j)} \geq 0$, $i, j = 1, \ldots, n$, $i \neq j$, where $A_{(i,j)}$ denotes the (i, j)th entry of A.

In this paper, we consider controlled nonlinear dynamical systems of the form

$$\dot{x}(t) = f(x(t)) + G(x(t))u(t), \ \ x(0) = x_0, \ \ t \geq 0 \tag{1}$$

where $x(t) \in \mathbb{R}^n$, $t \geq 0$, $u(t) \in \mathbb{R}^m$, $t \geq 0$, $f : \mathbb{R}^n \to \mathbb{R}^n$ is continuous and satisfies $f(0) = 0$, $G : \mathbb{R}^n \to \mathbb{R}^{n\times m}$ is continuous, and $u : [0, \infty) \to \mathbb{R}^m$ is measurable and locally bounded. For the nonnegative system (1), we assume that $f(\cdot)$, $G(\cdot)$, and $u(\cdot)$ satisfy sufficient regularity conditions such that (1) has a unique solution forward in time.

The following definition and proposition are needed for the main results of this paper.

Definition 3: The nonlinear dynamical system given by (1) is *nonnegative* if, for every $x(0) \in \overline{\mathbb{R}}_+^n$ and $u(t) \geq\geq 0$, $t \geq 0$, the solution $x(t)$, $t \geq 0$, to (1) is nonnegative.

[1] In this paper, it is important to distinguish between a square nonnegative (resp., positive) matrix and a nonnegative-definite (resp., positive-definite) matrix.

Proposition 1 ([28], [29]): The nonlinear dynamical system given by (1) is nonnegative if $f : \mathbb{R}^n \to \mathbb{R}^n$ is essentially nonnegative and $G(x) \geq\geq 0$, $x \in \overline{\mathbb{R}}_+^n$.

It follows from Proposition 1 that, if $f(\cdot)$ is essentially nonnegative, then a nonnegative input signal $G(x(t))u(t)$, $t \geq 0$, is sufficient to guarantee the nonnegativity of the state of (1).

III. Neuroadaptive Output Feedback Control with Actuator Constraints

In this section, we consider the problem of characterizing neuroadaptive dynamic output feedback control laws for nonlinear uncertain dynamical systems with actuator amplitude and integral constraints to achieve reference model output tracking. While our framework is applicable to general nonnegative and compartmental dynamical systems [29] with actuator amplitude and integral constraints, the main focus of this paper is the application of this framework to pressure-limited and work-limited control of mechanical ventilation. In this section, however, we present a general neuroadaptive control framework for nonlinear nonnegative dynamical systems with actuator amplitude and integral constraints.

Consider the controlled nonlinear uncertain dynamical system $\mathcal{G}$ given by

$$\dot{x}(t) = A_0 x(t) + B\Lambda f(x(t), h(u(t)), \theta(t)) + B\Lambda h(u(t)), \quad x(0) = x_0, \quad t \geq 0 \tag{2}$$

$$y(t) = Cx(t) \tag{3}$$

where $x(t) \in \mathbb{R}^n$, $t \geq 0$, is the state vector, $u(t) \in \mathbb{R}^m$, $t \geq 0$, is the control input, $y(t) \in \mathbb{R}^m$, $t \geq 0$, is the system output, $A_0 \in \mathbb{R}^{n\times n}$ is a nominal known Hurwitz and essentially nonnegative matrix, $B \in \mathbb{R}^{r\times m}$ is a known nonnegative input matrix, $\Lambda \in \mathbb{R}^{m\times m}$ is an *unknown* nonnegative and positive-definite matrix, $h(u(t)) = [h_1(u_1(t)), \ldots, h_m(u_m(t))]^{\mathrm{T}}$ is the constrained control input given by

$$h_i(u_i) \triangleq \begin{cases} 0, & \text{if } u_i \leq 0, \\ u_i^*, & \text{if } u_i \geq u_i^*, \\ u_i, & \text{otherwise} \end{cases} \tag{4}$$

where $u_i^* > 0$, $i = 1, \ldots, m$, are given constants, $\theta : \mathbb{R} \to \mathcal{D}_\theta$ is a known bounded continuous function, where $\mathcal{D}_\theta \subset \mathbb{R}$ is a compact set, $f : \mathbb{R}^n \times \mathbb{R}^m \times \mathcal{D}_\theta \to \mathbb{R}^m$ is Lipschitz continuous and essentially nonnegative for all $u \in \mathbb{R}^m$ and $\theta \in \mathcal{D}_\theta$ but otherwise *unknown* (that is, $f(\cdot, \cdot, \cdot)$ is such that $f_i(x, h(u), \theta) \geq 0$ if $x_i = 0$, $i = 1, \ldots, n$, for all $u \in \mathbb{R}^m$ and $\theta \in \mathcal{D}_\theta$), and $C \in \mathbb{R}^{m\times n}$ is a known output matrix.

For the mechanical ventilation problem, the control input $u(t)$, $t \geq 0$, represents the pressure input to the ventilator and the control input constraint (4) captures pressure amplitude limitations. Furthermore, as we see in Section V, the function $\theta(t)$, $t \geq 0$, is introduced to account for a continuous transition of the respiratory parameters (e.g., lung resistance and compliance) from inspiration to expiration. Finally, note that the system structure given by (2) involves a non-affine system in the control input. For details of such systems, see [30], [31].

In order to achieve output tracking, we construct a reference nonnegative dynamical system $\mathcal{G}_{\rm ref}$ given by

$$\dot{x}_{\rm ref}(t) = A_{\rm ref}x_{\rm ref}(t) + B_{\rm ref}r(t),\ x_{\rm ref}(0) = x_{{\rm ref}_0},\ t \geq 0 \quad (5)$$

$$y_{\rm ref}(t) = Cx_{\rm ref}(t) \quad (6)$$

where $x_{\rm ref}(t) \in \mathbb{R}^n$, $t \geq 0$, is the reference state vector, $r(t) \in \mathbb{R}^d$, $t \geq 0$, is a bounded piecewise continuous nonnegative reference input, $A_{\rm ref} \in \mathbb{R}^{n\times n}$ is a Hurwitz and essentially nonnegative matrix, and $B_{\rm ref} \in \mathbb{R}^{n\times d}$ is a nonnegative matrix.

Control (source) inputs for mechanical ventilation involving pressure control are usually constrained to be nonnegative as are the system states, which typically correspond to compartmental volumes. Hence, in this paper we develop neuroadaptive dynamic output feedback control laws for nonnegative systems with nonnegative control inputs. Specifically, for the reference model output tracking problem our goal is to design a nonnegative control input $u(t)$, $t \geq 0$, predicated on the system measurement $y(t)$, $t \geq 0$, such that $\|y(t)-y_{\rm ref}(t)\| < \gamma$ for all $t \geq T$, where $\|\cdot\|$ denotes the Euclidean vector norm on $\mathbb{R}^m$, $\gamma > 0$ is sufficiently small, and $T \in [0, \infty)$, $x(t) \geq\geq 0$, $t \geq 0$, for all $x_0 \in \overline{\mathbb{R}}^n_+$, and the control input $u(\cdot)$ in (2) is restricted to the class of *admissible controls* consisting of measurable functions $u(t) = [u_1(t), \ldots, u_m(t)]^{\rm T}$, $t \geq 0$, such that (4) holds and

$$\eta_i(t) \triangleq \int_{t-\tau_{\rm s}}^{t} h_i(u_i(s)){\rm d}s \leq \eta_i^*,\ \ i = 1, \ldots, m,\ \ t \geq 0 \quad (7)$$

where $\tau_{\rm s} > 0$ and $\eta_i^* > 0$, $i = 1, \ldots, m$, are given constants and $u_i(t) \equiv 0$ for all $t \in [-\tau_{\rm s}, 0]$ and $i = 1, \ldots, m$. Note that $\eta_i(t)$, $i = 1, \ldots, m$, $t \geq 0$, given by (7), satisfies

$$\dot{\eta}_i(t) = h_i(u_i(t)) - h_i(u_i(t-\tau_{\rm s})),\ \ \eta_i(0) = 0,\ \ t \geq 0. \quad (8)$$

For the mechanical ventilation problem, the pressure control integral constraint (7) enforces an upper bound on the amount of work performed by the ventilator.

Here, we assume that the function $f(x, h(u), \theta)$ can be approximated over a compact set $\mathcal{D}_x \times \mathcal{D}_u \times \mathcal{D}_\theta$ by a linear in parameters neural network up to a desired accuracy. In this case, there exists $\hat{\varepsilon} : \mathbb{R}^n \times \mathbb{R}^m \times \mathcal{D}_\theta \to \mathbb{R}^m$ such that $\|\hat{\varepsilon}(x, h(u), \theta)\| < \hat{\varepsilon}^*$ for all $(x, h(u), \theta) \in \mathcal{D}_x \times \mathcal{D}_u \times \mathcal{D}_\theta$, where $\hat{\varepsilon}^* > 0$, and

$$f(x, h(u), \theta) = W_f^{\rm T}\hat{\sigma}(x, u, \theta) + \hat{\varepsilon}(x, u, \theta),\quad (x, u, \theta) \in \mathcal{D}_x \times \mathcal{D}_u \times \mathcal{D}_\theta \quad (9)$$

where $W_f \in \mathbb{R}^{s\times m}$ is an optimal *unknown* (constant) weight that minimizes the approximation error over $\mathcal{D}_x \times \mathcal{D}_u \times \mathcal{D}_\theta$, $\hat{\sigma} : \mathbb{R}^n \times \mathbb{R}^m \times \mathcal{D}_\theta \to \mathbb{R}^s$ is a vector of basis functions such that each component of $\hat{\sigma}(\cdot, \cdot, \cdot)$ takes values between 0 and 1, and $\hat{\varepsilon}(\cdot, \cdot, \cdot)$ is the modeling error. Note that s denotes the number of basis functions or equivalently, the number of nodes of the neural network approximating the nonlinear function $f(x, h(u), \theta)$ on a compact set $(x, u, \theta) \in \mathcal{D}_x \times \mathcal{D}_u \times \mathcal{D}_\theta$.

Since $f(\cdot, \cdot, \cdot)$ is continuous on $\mathbb{R}^n \times \mathbb{R}^m \times \mathcal{D}_\theta$, we can choose $\hat{\sigma}(\cdot, \cdot, \cdot)$ from a linear space $\mathcal{X}$ of continuous functions that forms an algebra and separates points in $\mathcal{D}_x \times \mathcal{D}_u \times \mathcal{D}_\theta$. In this case, it follows from the Stone–Weierstrass theorem [32, p. 212] that $\mathcal{X}$ is a dense subset of the set of continuous functions on $\mathcal{D}_x \times \mathcal{D}_u \times \mathcal{D}_\theta$. Now, as is the case in the standard neuroadaptive control literature [33], we can construct a signal involving the estimates of the optimal weights and basis functions as our adaptive control signal. It is important to note here that we assume that we know the structure and the size of the approximator. This is a standard assumption in the neural network adaptive control literature. In online neural network training, the size and the structure of the optimal approximator are not known and are often chosen by the rule that the larger the size of the neural network and the richer the distribution class of the basis functions over a compact domain, the tighter the resulting approximation error bound $\hat{\varepsilon}(\cdot, \cdot, \cdot)$. This goes back to the Stone–Weierstrass theorem which only provides an existence result without any constructive guidelines.

In order to develop an *output* feedback neuroadaptive controller, we use the approach developed in [34] for reconstructing the system states via the system delayed inputs and outputs. Specifically, we use a *memory unit* as a particular form of a tapped delay line (TDL), which takes a scalar time series input and provides an $(2mn - r)$-dimensional vector output consisting of the present values of the system outputs and system inputs, and their $2(n - 1)m - r$ delayed values given by

$$\begin{aligned}\kappa(t) \triangleq\ & [y_1(t), y_1(t-d), \ldots, y_1(t-(n-1)d), \ldots,\\ & y_m(t), y_m(t-d), \ldots, y_m(t-(n-1)d);\\ & u_1(t), u_1(t-d), \ldots, u_1(t-(n-r_1-1)d),\\ & \ldots, u_m(t), u_m(t-d), \ldots,\\ & u_m(t-(n-r_m-1)d)]^{\rm T}\quad t \geq 0\end{aligned} \quad (10)$$

where r_i denotes the relative degree of $\mathcal{G}$ with respect to the output y_i, $i = 1, \ldots, m$, and $r \triangleq r_1 + \cdots + r_m$ denotes the (vector) relative degree of $\mathcal{G}$.

The following matching conditions are needed for the main result of this paper.

Assumption 1: There exist $K_{\rm y} \in \mathbb{R}^{m\times m}$ and $K_{\rm r} \in \mathbb{R}^{m\times d}$ such that $A_0 + BK_{\rm y}C = A_{\rm ref}$ and $BK_{\rm r} = B_{\rm ref}$.

Assumption 1 involves standard matching conditions for model reference adaptive control appearing in the literature, see, for example [35, Ch. 5].

Using the parameterization $\Lambda = \hat{\Lambda} + \Delta\Lambda$, where $\Delta\Lambda \in \mathbb{R}^{m\times m}$ is an unknown symmetric matrix, the dynamics in (2) can be rewritten as

$$\begin{aligned}\dot{x}(t) =\ & A_0x(t) + B\hat{\Lambda}h(u(t)) + B[\Delta\Lambda h(u(t))\\ & +\Lambda f(x(t), h(u(t)), \theta(t))],\ \ x(0) = x_0,\ \ t \geq 0.\end{aligned} \quad (11)$$

Define $W \triangleq \left[W_1^{\rm T}, W_2^{\rm T}\right]^{\rm T} \in \mathbb{R}^{(s+m)\times m}$, where $W_1 \triangleq W_f\Lambda$ and $W_2 \triangleq \Delta\Lambda^{\rm T}$, and $\zeta(t) \triangleq \left[\kappa^{\rm T}(t), \theta(t)\right]^{\rm T}$, $t \geq 0$. Using (9), (11) can be rewritten as

$$\begin{aligned}\dot{x}(t) =\ & A_0x(t) + B\hat{\Lambda}u(t) + BW^{\rm T}\sigma(\zeta(t), h(u(t)))\\ & + B\ \Lambda\hat{\varepsilon}(x(t), u(t), \theta(t)) + B\ \hat{\Lambda}\Delta h(t)\\ & + B\ W_1^{\rm T}\left[\hat{\sigma}(x(t), u(t), \theta(t)) - \sigma_\zeta(\zeta(t))\right],\\ & x(0) = x_0,\quad t \geq 0\end{aligned} \quad (12)$$

where

$$\sigma(\zeta(t), h(u(t))) \triangleq \left[\sigma_\zeta^{\rm T}(\zeta(t)), h^{\rm T}(u(t))\right]^{\rm T} \quad (13)$$

$\sigma_\zeta : \mathbb{R}^{2mn-r+1} \to \mathbb{R}^s$ is a vector of basis functions such that each component of $\sigma_\zeta(\cdot)$ takes values between 0 and 1, and $\Delta h(u(t)) \triangleq h(u(t)) - u(t)$, $t \geq 0$.

Next, consider a sequence of positive numbers $\{\rho_i\}_{i=1}^{\infty}$ such that $\lim_{i\to\infty} \rho_i = 0$ and define the time-dependent set $\mathbf{\Omega}_{t,i}$ and *saturation impact times* $\tau_i^*(t)$ by

$$\mathbf{\Omega}_{t,i} \triangleq \{\tau \geq 0 : \eta_i(\tau) = \eta_i^* \text{ and there exists } N > 0 \text{ such that for all } i \geq N,\ \eta_i(\tau - \rho_i) < \eta_i^*\}, \quad t \geq 0, \quad i = 1, \ldots, m \tag{14}$$

$$\tau_i^*(t) \triangleq \begin{cases} \theta_i + \max\{\tau : \tau \in \mathbf{\Omega}_{t,i}\}, & \text{if } \mathbf{\Omega}_{t,i} \neq \varnothing, \\ 0, & \text{otherwise,} \end{cases} \quad t \geq 0, \quad i = 1, \ldots, m \tag{15}$$

where $\theta_i > 0$, $i = 1, \ldots, m$, are design parameters.

Now, consider the control input $u(t)$, $t \geq 0$, given by

$$u(t) = \Phi(\eta(t))\psi(t), \quad t \geq 0 \tag{16}$$

where $\Phi(\eta(t)) \triangleq \text{diag}\,[\phi_1(\eta_1(t)), \ldots, \phi_m(\eta_m(t))]$, $t \geq 0$

$$\phi_i(\eta_i(t)) \triangleq \begin{cases} 1, & \text{if } 0 \leq \eta_i(t) \leq \eta_i^* - \delta_i \text{ and } t \geq \tau_i^*(t), \\ \frac{1}{\delta_i}(\eta_i^* - \eta_i(t)), & \text{if } \eta_i^* - \delta_i \leq \eta_i(t) \leq \eta_i^*, \text{ and } t \geq \tau_i^*(t) \\ 0, & \text{otherwise} \end{cases} \quad t \geq 0, \quad i = 1, \ldots, m. \tag{17}$$

$0 < \delta_i < \eta_i^*$, $i = 1, \ldots, m$, are design constant parameters (chosen to be sufficiently small), and $\psi(t) \in \mathbb{R}^m$, $t \geq 0$, is given by

$$\psi(t) = \psi_{\rm n}(t) - \psi_{\rm ad}(t), \quad t \geq 0 \tag{18}$$

where

$$\psi_{\rm n}(t) = \hat{\Lambda}^{-1}[K_{\rm y}y(t) + K_{\rm r}r(t)], \quad t \geq 0 \tag{19}$$

$$\psi_{\rm ad}(t) = \hat{\Lambda}^{-1}\hat{W}^{\rm T}(t)\sigma(\zeta(t), h(u(t))), \quad t \geq 0 \tag{20}$$

and $\hat{W}(t) \in \mathbb{R}^{(s+m)\times m}$, $t \geq 0$, is an update weight. Note that, for all $t \geq 0$ and $i = 1, \ldots, m$, $0 \leq \phi_i(\eta_i(t)) \leq 1$. Furthermore, if $\eta_i(\hat{t}) = \eta_i^*$ for every $\hat{t} \geq 0$, then $h_i(u_i(\hat{t})) = 0$. Now, it follows from (8) that $\dot{\eta}(\hat{t}) = -h_i(u_i(\hat{t} - \tau_{\rm s})) \leq 0$, $\hat{t} \geq 0$, and hence, $\eta_i(\hat{t})$ is upper bounded by η_i^*. Thus, the integral constraint (7) is satisfied. Fig. 1 shows the interplay between $\eta_i(t)$ and $\phi_i(\eta_i(t))$, $i = 1, \ldots, m$.

Remark 1: The choice of $\phi_i(\eta_i)$, $i = 1, \ldots, m$, is not limited to the piecewise linear continuous function given by (17). In particular, on the interval $\eta_i^* - \delta_i \leq \eta_i \leq \eta_i^*$, $\phi_i(\eta_i)$ can be chosen as any decreasing continuous function such that $\phi_i(\eta_i^* - \delta_i) = 1$ and $\phi_i(\eta_i^*) = 0$.

Defining the tracking error state $e(t) \triangleq x(t) - x_{\rm ref}(t)$, $t \geq 0$, and using (16), (18)–(20), and Assumption 1, the error dynamics is given by

$$\dot{e}(t) = A_{\rm ref}e(t) + B\tilde{W}^{\rm T}(t)\sigma(\zeta(t), h(u(t))) + B\hat{\Lambda}\Delta h(u(t)) + \varepsilon(t), \; e(0) = x_0 - x_{\rm ref_0}, \; t \geq 0 \tag{21}$$

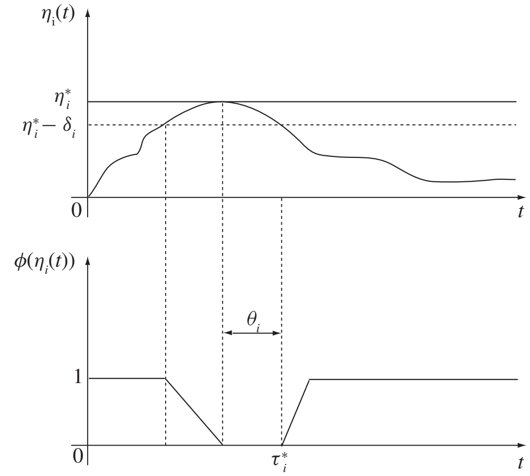

Fig. 1. Visualization of the effect of $\phi_i(\eta_i(t))$ for a given function $\eta_i(t)$.

where

$$\varepsilon(t) \triangleq B\hat{\Lambda}(\Phi(t) - I_m)\psi(t) + BW_1^{\rm T}[\hat{\sigma}(x(t), u(t), \theta(t)) - \sigma_\zeta(\zeta(t))] + B\Lambda\hat{\varepsilon}(x(t), u(t), \theta(t))$$

and $\tilde{W}(t) \triangleq W - \hat{W}(t)$, $t \geq 0$.

Next, to account for the effects of saturation (pressure limitation) on the error state $e(t)$, $t \geq 0$, consider the dynamical system given by

$$\dot{e}_{\rm s}(t) = A_{\rm ref}e_{\rm s}(t) + B\hat{\Lambda}\Delta h(u(t)), e_{\rm s}(0) = e_{\rm s0}, \; t \geq 0 \tag{22}$$

$$y_{\rm s}(t) = Ce_{\rm s}(t) \tag{23}$$

where $e_{\rm s}(t) \in \mathbb{R}^n$, $t \geq 0$, and define the shifted error state $\tilde{e}(t) \triangleq e(t) - e_{\rm s}(t)$, $t \geq 0$. Now, it follows from (21) and (22) that

$$\dot{\tilde{e}}(t) = A_{\rm ref}\tilde{e}(t) + B\tilde{W}^{\rm T}(t)\sigma(\zeta(t), h(u(t))) + \varepsilon(t), \quad \tilde{e}(0) = 0, \quad t \geq 0. \tag{24}$$

For the statement of the main result, define the projection operator $\text{Proj}(\tilde{W}, Y)$ by

$$\text{Proj}(\tilde{W}, Y) \triangleq \begin{cases} Y, & \text{if } \mu(\tilde{W}) < 0, \\ Y, & \text{if } \mu(\tilde{W}) \geq 0 \text{ and } \mu'(\tilde{W})Y \leq 0, \\ Y - \frac{\mu'^{\rm T}(\tilde{W})\mu'(\tilde{W})Y}{\mu'(\tilde{W})\mu'^{\rm T}(\tilde{W})}\mu(\tilde{W}), & \text{otherwise} \end{cases}$$

where $\tilde{W} \in \mathbb{R}^{s\times m}$, $Y \in \mathbb{R}^{n\times m}$, $\mu(\tilde{W}) \triangleq (\text{tr}\,\tilde{W}^{\rm T}\tilde{W} - \tilde{w}_{\max}^2)/\varepsilon_{\tilde{W}}$, $\tilde{w}_{\max} \in \mathbb{R}$ is the norm bound imposed on $\tilde{W}$, and $\varepsilon_{\tilde{W}} > 0$. Note that for a given matrix $\tilde{W} \in \mathbb{R}^{s\times m}$ and $Y \in \mathbb{R}^{n\times m}$, it follows that

$$\text{tr}[(\tilde{W} - W)^{\rm T}(\text{Proj}(\tilde{W}, Y) - Y)] = \sum_{i=1}^{n}[\text{col}_i(\tilde{W} - W)]^{\rm T}[\text{Proj}(\text{col}_i(\tilde{W}), \text{col}_i(Y)) - \text{col}_i(Y)] \leq 0$$

where $\text{col}_i(X)$ denotes the ith column of the matrix X.

Consider the update law given by

$$\dot{\hat{W}}(t) = \Gamma_W \mathrm{Proj}[\hat{W}(t), \sigma(\zeta(t), h(u(t)))\xi_c^{\mathrm{T}}(t)PB], \quad \hat{W}(0) = \hat{W}_0, \ t \geq 0 \tag{25}$$

where $\Gamma_W \in \mathbb{R}^{(s+m)\times(s+m)}$ is a positive definite matrix, $P \in \mathbb{R}^{n\times n}$ is a positive-definite solution of the Lyapunov equation

$$0 = A_{\mathrm{ref}}^{\mathrm{T}} P + P A_{\mathrm{ref}} + R \tag{26}$$

where $R > 0$, and $\xi_c(t) \in \mathbb{R}^{n_\xi}$, $t \geq 0$, is the solution to the estimator dynamics

$$\dot{\xi}_c(t) = \hat{A}\xi_c(t) + L\left[y(t) - y_{\mathrm{ref}}(t) - y_c(t) - y_s(t)\right], \quad \xi_c(0) = \xi_{c0}, \quad t \geq 0 \tag{27}$$

$$y_c(t) = \hat{C}\xi_c(t) \tag{28}$$

where $\hat{A} \in \mathbb{R}^{n_\xi \times n_\xi}$ is Hurwitz, $L \in \mathbb{R}^{n_\xi \times m}$, and $\hat{C} \in \mathbb{R}^{m\times n_\xi}$. In addition, let $\tilde{P} \in \mathbb{R}^{n_\xi \times n_\xi}$ be a positive-definite solution of the Lyapunov equation

$$0 = (\hat{A} - L\hat{C})^{\mathrm{T}}\tilde{P} + \tilde{P}(\hat{A} - L\hat{C}) + \tilde{R} \tag{29}$$

where $\tilde{R} > 0$.

Now, since the projection operator used in the update law (25) guarantees the boundness of the update weight $\hat{W}(t)$, $t \geq 0$, it follows that there exist $u^* > 0$ and $\delta^* > 0$ such that $\|u(t)\| \leq u^*$ and $\|\Delta h(u(t))\| \leq \delta^*$ for all $t \geq 0$. Furthermore, note that there exists $\varepsilon^* > 0$ such that $\|\varepsilon(t)\| \leq \varepsilon^*$ for all $t \geq 0$ and $(x(t), u(t), \theta(t)) \in \mathcal{D}_x \times \mathcal{D}_u \times \mathcal{D}_\theta$. Finally, there exists $\alpha_1 > 0$ such that $\|\tilde{W}^{\mathrm{T}}(t)\sigma(\zeta(t), h(u(t)))\| \leq \alpha_1$ for all $t \geq 0$.

For the statement of the main result of this paper, let $\|\cdot\|' : \mathbb{R}^{n\times n} \to \mathbb{R}$ be the matrix norm equi-induced by the vector norm $\|\cdot\|'' : \mathbb{R}^n \to \mathbb{R}$, let $\|\cdot\|''' : \mathbb{R}^{n\times m} \to \mathbb{R}$ be the matrix norm induced by the vector norms $\|\cdot\|'' : \mathbb{R}^n \to \mathbb{R}$ and $\|\cdot\|'''' : \mathbb{R}^m \to \mathbb{R}$, and let $\|\cdot\|^* : \mathbb{R}^{n_\xi \times n_\xi} \to \mathbb{R}$ be the matrix norm equi-induced by the vector norm $\|\cdot\|^{**} : \mathbb{R}^{n_\xi} \to \mathbb{R}$. Furthermore, recall the definition of ultimate boundness of a state trajectory given in [36, p. 241].

Theorem 1: Consider the nonlinear uncertain dynamical system $\mathcal{G}$ given by (2) and (3) with $u(t)$, $t \geq 0$, given by (16)–(20) and reference model $\mathcal{G}_{\mathrm{ref}}$ given by (5) and (6) with tracking error dynamics given by (21). Assume Assumption 1 holds, $\lambda_{\min}(R) > 1$, and $\lambda_{\min}(\tilde{R}) > \|\tilde{P}L\hat{C}\|^{*2}$. Then there exists a compact positively invariant set $\mathcal{D}_\alpha \subset \mathbb{R}^n \times \mathbb{R}^n \times \mathbb{R}^{n_\xi} \times \mathbb{R}^{(s+m)\times m}$ such that $(0, 0, 0, W) \in \mathcal{D}_\alpha$, where $W \in \mathbb{R}^{(s+m)\times m}$, and the solution $(e(t), e_s(t), \xi_c(t), \hat{W}(t))$, $t \geq 0$, of the closed-loop system given by (2), (3), (16), (22), (23), (25), (27), and (28) is ultimately bounded for all $(e(0), e_s(0), \xi_c(0), \hat{W}(0)) \in \mathcal{D}_\alpha$ with ultimate bound $\|y(t) - y_{\mathrm{ref}}(t)\| < \gamma$, $t \geq T$, where

$$\gamma > \left(\left[(\lambda_{\min}(R) - 1)^{-\frac{1}{2}}\sqrt{\nu} + \alpha_e\right]^2 + \left[(\lambda_{\min}(\tilde{R}) - \|\tilde{P}L\hat{C}\|^{*2})^{-\frac{1}{2}}\sqrt{\nu} + \alpha_\xi\right]^2 + \lambda_{\max}(\Gamma_W^{-1})\hat{w}^2{}_{\max}\right)^{\frac{1}{2}} \tag{30}$$

$$\nu \triangleq (\lambda_{\min}(R) - 1)\alpha_e^2 + (\lambda_{\min}(\tilde{R}) - \|\tilde{P}L\hat{C}\|^{*2})\alpha_\xi^2 \tag{31}$$

$$\alpha_e \triangleq \frac{1}{\lambda_{\min}(R) - 1}\left(\|P\|'\varepsilon^* + \|PB\|'''\alpha_1\right) \tag{32}$$

$$\alpha_\xi \triangleq \frac{1}{\lambda_{\min}(\tilde{R}) - \|\tilde{P}L\hat{C}\|^{*2}}\|PB\|'''\alpha_1 \tag{33}$$

and $\hat{w}_{\max}$ is a norm bound imposed on $\hat{W}$. Furthermore, $u(t)$ satisfies (7) for all $t \geq 0$, $h(u(t)) \geq\geq 0$, $t \geq 0$, and $x(t) \geq\geq 0$, $t \geq 0$, for all $x_0 \in \overline{\mathbb{R}}_+^n$.

Proof: Ultimate boundness of the closed-loop system follows by considering the Lyapunov-like function candidate

$$V(\tilde{e}, \xi_c, \tilde{W}) = \tilde{e}^{\mathrm{T}}P\tilde{e} + \xi_c^{\mathrm{T}}\tilde{P}\xi_c + \mathrm{tr}\,\tilde{W}^{\mathrm{T}}\Gamma_W^{-1}\tilde{W} \tag{34}$$

where $P > 0$ and $\tilde{P} > 0$ satisfy, respectively, (26) and (29). Note that (34) satisfies $\alpha(\|z\|) \leq V(z) \leq \beta(\|z\|)$ with $z = [\tilde{e}^{\mathrm{T}}, \xi_c^{\mathrm{T}}, (\mathrm{vec}\,\tilde{W})^{\mathrm{T}}]^{\mathrm{T}}$ and $\alpha(\|z\|) = \beta(\|z\|) = \|z\|^2$, where $\|z\|^2 \triangleq \tilde{e}^{\mathrm{T}}P\tilde{e} + \xi_c^{\mathrm{T}}\tilde{P}\xi_c + \mathrm{tr}\,\tilde{W}^{\mathrm{T}}\Gamma_W^{-1}\tilde{W}$ and $\mathrm{vec}(\cdot)$ denotes the column stacking operator. Furthermore, note that $\alpha(\|z\|)$ is a class $\mathcal{K}_\infty$ function [36]. Now, using (25), and after considerable, albeit standard, algebraic manipulations (see [24], [37] for similar details), the time derivative of $V(\tilde{e}, \xi_c, \tilde{W})$ along the closed-loop system trajectories satisfies

$$\dot{V}(\tilde{e}(t), \xi_c(t), \tilde{W}(t)) \leq -\left(\lambda_{\min}(RP^{-1}) - 1\right)(\|\tilde{e}(t)\| - \alpha_e)^2 + \nu - \left(\lambda_{\min}(\tilde{R}) - \|\tilde{P}L\hat{C}\|^{*2}\right)\left(\|\xi_c(t)\| - \alpha_\xi\right)^2, \ t \geq 0. \tag{35}$$

Now, for

$$\|\tilde{e}\| \geq \alpha_{\tilde{e}} \triangleq \sqrt{\frac{\nu}{\lambda_{\min}(RP^{-1}) - 1}} + \alpha_e \tag{36}$$

or

$$\|\xi_c\| \geq \alpha_{\xi_c} \triangleq \sqrt{\frac{\nu}{\lambda_{\min}(\tilde{R}) - \|\tilde{P}L\hat{C}\|^{*2}}} + \alpha_\xi \tag{37}$$

it follows that $\dot{V}(\tilde{e}(t), \xi_c(t), \tilde{W}(t)) \leq 0$ for all $t \geq 0$, that is, $\dot{V}(\tilde{e}(t), \xi_c(t), \tilde{W}(t)) \leq 0$ for all $(\tilde{e}(t), \xi_c(t), \tilde{W}(t)) \in \tilde{\mathcal{D}}_e \backslash \tilde{\mathcal{D}}_r$ and $t \geq 0$, where

$$\tilde{\mathcal{D}}_e \triangleq \Big\{(\tilde{e}, \xi_c, \tilde{W}) \in \mathbb{R}^n \times \mathbb{R}^{n_\xi} \times \mathbb{R}^{(s+m)\times m} : (x, \hat{u}, \theta) \in \mathcal{D}_x \times \mathcal{D}_{\hat{u}} \times \mathcal{D}_\theta\Big\} \tag{38}$$

$$\tilde{\mathcal{D}}_r \triangleq \Big\{(\tilde{e}, \xi_c, \tilde{W}) \in \mathbb{R}^n \times \mathbb{R}^{n_\xi} \times \mathbb{R}^{(s+m)\times m} : \|\tilde{e}\| \leq \alpha_{\tilde{e}} \text{ or } \|\xi_c\| \leq \alpha_{\xi_c}\Big\}. \tag{39}$$

Next, define

$$\tilde{\mathcal{D}}_\alpha \triangleq \Big\{(\tilde{e}, \xi_c, \tilde{W}) \in \mathbb{R}^n \times \mathbb{R}^{n_\xi} \times \mathbb{R}^{(s+m)\times m} : V(\tilde{e}, \xi_c, \tilde{W}) \leq \alpha\Big\} \tag{40}$$

where α is the maximum value such that $\tilde{\mathcal{D}}_\alpha \subseteq \tilde{\mathcal{D}}_e$, and define

$$\tilde{\mathcal{D}}_\eta \triangleq \Big\{(\tilde{e}, \xi_c, \tilde{W}) \in \mathbb{R}^n \times \mathbb{R}^{n_\xi} \times \mathbb{R}^{(s+m)\times m} : V(\tilde{e}, \xi_c, \tilde{W}) \leq \eta\Big\} \tag{41}$$

where

$$\eta > \beta(\mu) = \mu = \alpha_{\tilde{e}}^2 + \alpha_{\xi_c}^2 + \lambda_{\max}(\Gamma_W^{-1})\hat{w}^2{}_{\max}. \tag{42}$$

To show ultimate boundedness of the closed-loop system (2)–(3), (16), (22)–(25), (27), and (28) assume[2] that $\tilde{\mathcal{D}}_\eta \subset \tilde{\mathcal{D}}_\alpha$.

[2]This assumption is standard in the neural network literature and ensures that in the error space $\tilde{\mathcal{D}}_e$ there exists at least one Lyapunov level set $\tilde{\mathcal{D}}_\eta \subset \tilde{\mathcal{D}}_\alpha$. Equivalently, imposing bounds on the adaptation gains ensures $\tilde{\mathcal{D}}_\eta \subset \tilde{\mathcal{D}}_\alpha$ [38]. In the case where the neural network approximation holds in $\mathbb{R}^n$ with delayed values, this assumption is automatically satisfied.

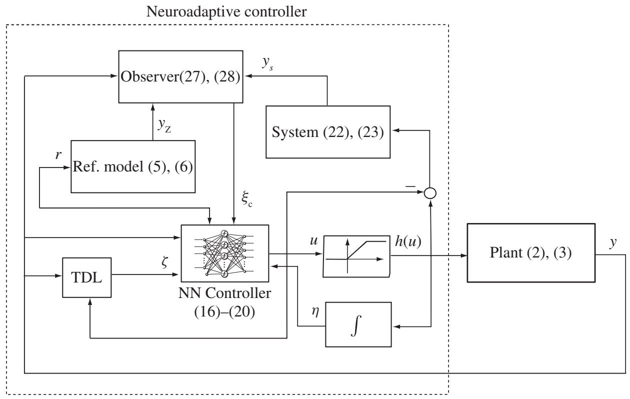

Fig. 2. Block diagram of the closed-loop system.

Now, since $\dot{V}(\tilde{e}, \xi_c, \tilde{W}) \leq 0$ for all $(\tilde{e}, \xi_c, \tilde{W}) \in \tilde{\mathcal{D}}_e \backslash \tilde{\mathcal{D}}_r$ and $\tilde{\mathcal{D}}_r \subset \tilde{\mathcal{D}}_\alpha$, it follows that $\tilde{\mathcal{D}}_\alpha$ is positively invariant. Hence, if $(\tilde{e}(0), \xi_c(0), \tilde{W}(0)) \in \tilde{\mathcal{D}}_\alpha$, then it follows from [36, Corr. 4] that the solution $(\tilde{e}(t), \xi_c(t), \tilde{W}(t))$, $t \geq 0$, to (24), (25), (27), and (28) is ultimately bounded with ultimate bound given by $\gamma = \alpha^{-1}(\eta) = \sqrt{\eta}$, which yields (30).

The nonnegativity of $h(u(t))$, $t \geq 0$, is immediate from (4). The fact that $u(t)$, $t \geq 0$, satisfies (7) follows from (16), (17), and the fact that $h(u) \geq\geq 0$ for all $u \in \mathbb{R}^m$. Since A_0 is essentially nonnegative, $B\Lambda \geq\geq 0$, $h(u(t)) \geq\geq 0$, $t \geq 0$, and $f(x, h(u), \theta)$ is essentially nonnegative for all $u \in \mathbb{R}^m$ and $\theta \in \mathcal{D}_\theta$, it follows from (2) and Proposition 1 that $x(t) \geq\geq 0$, $t \geq 0$, for all $x_0 \in \overline{\mathbb{R}}^n_+$. This completes the proof. ■

A block diagram showing the neuroadaptive control architecture given in Theorem 1 is shown in Fig. 2.

Remark 2: To apply Theorem 1 to a set-point regulation problem, let $x_e \in \overline{\mathbb{R}}^n_+$ and $r(t) \equiv r^*$ be such that $0 = A_{\rm ref} x_e + B_{\rm ref} r^*$ and $y_{\rm ref}(t) \equiv y_d = C x_e$, where $y_d \in \overline{\mathbb{R}}^m_+$ is a given desired set-point. In this case, the control signal $u(t)$ is given by (16) and (18) with $\psi_n(t) \equiv 0$.

IV. Nonlinear Multicompartment Model for a Pressure-Limited Respirator

In this section, we extend the linear multicompartment lung model of [27] to develop a nonlinear model for the dynamic behavior of a multicompartment respiratory system in response to an arbitrary applied inspiratory pressure. Here we assume that the bronchial tree has a dichotomy architecture [39], that is, in every generation each airway unit branches in two airway units of the subsequent generation. In addition, we assume that lung compliance is a nonlinear function of lung volume. First, for simplicity of exposition, we consider a single-compartment lung model as shown in Fig. 3.

In this model, the lungs are represented as a single lung unit with nonlinear compliance $c(x)$ connected to a pressure source by an airway unit with resistance (to air flow) of R. At time $t = 0$, an arbitrary pressure $p_{\rm in}(t)$ is applied to the opening of the parent airway, where $p_{\rm in}(t)$ is determined by the mechanical ventilator. This pressure is applied to the airway opening over the time interval $0 \leq t \leq T_{\rm in}$, which is the inspiratory part of the breathing cycle. At time $t = T_{\rm in}$, the applied airway pressure is released and expiration takes place

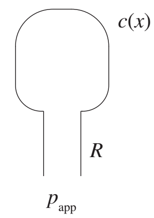

Fig. 3. Single-compartment lung model.

passively, that is, the external pressure is only the atmospheric pressure $p_{\rm ex}(t)$ during the time interval $T_{\rm in} \leq t \leq T_{\rm in} + T_{\rm ex}$, where $T_{\rm ex}$ is the duration of expiration.

The state equation for inspiration (inflation of lung) is given by

$$R_{\rm in}\dot{x}(t) + \frac{1}{c_{\rm in}(x)} x(t) = p_{\rm in}(t),\, x(0) = x_0^{\rm in},\ \ 0 \leq t \leq T_{\rm in} \quad (43)$$

where $x(t) \in \mathbb{R}$, $t \geq 0$, is the lung volume, $R_{\rm in} \in \mathbb{R}$ is the resistance to air flow during the inspiration period, $c_{\rm in} : \mathbb{R} \rightarrow \mathbb{R}_+$ is a nonlinear function defining the lung compliance at inspiration, $x_0^{\rm in} \in \mathbb{R}_+$ is the lung volume at the start of the inspiration and serves as the system initial condition. Equation (43) is simply a pressure balance equation where the total pressure $p_{\rm in}(t), t \geq 0$, applied to the compartment is proportional to the volume of the compartment via the compliance and the rate of change of the compartmental volume via the resistance. We assume that expiration is passive (due to elastic stretch of lung unit). During the expiration process, the state equation is given by

$$R_{\rm ex}\dot{x}(t) + \frac{1}{c_{\rm ex}(x)} x(t) = p_{\rm ex}(t),\ \ x(T_{\rm in}) = x_0^{\rm ex},$$
$$T_{\rm in} \leq t \leq T_{\rm in} + T_{\rm ex} \quad (44)$$

where $x(t) \in \mathbb{R}$, $t \geq 0$, is the lung volume, $R_{\rm ex} \in \mathbb{R}$ is the resistance to air flow during the expiration period, $c_{\rm ex} : \mathbb{R} \rightarrow \mathbb{R}_+$ is a nonlinear function defining the lung compliance at expiration, and $x_0^{\rm ex} \in \mathbb{R}_+$ is the lung volume at the start of expiration.

Next, we develop the state equations for inspiration and expiration for a 2^n-compartment model, where $n \geq 0$. In this model, the lungs are represented as 2^n lung units which are connected to the pressure source by n generations of airway units, where each airway is divided into two airways of the subsequent generation leading to 2^n compartments (see Fig. 4 for a four-compartment model).

Let x_i, $i = 1, 2, \ldots, 2^n$, denote the lung volume in the ith compartment, $c_i^{\rm in}(x_i)$, $i = 1, 2, \ldots, 2^n$, denote the compliance of each compartment as a nonlinear function of the volume of ith compartment, and let $R_{j,i}^{\rm in}$ (resp., $R_{j,i}^{\rm ex}$), $i = 1, 2, \ldots, 2^j$, $j = 0, \ldots, n$, denote the resistance (to air flow) of the ith airway in the jth generation during the inspiration (resp., expiration) period with $R_{01}^{\rm in}$ (resp., $R_{01}^{\rm ex}$) denoting the inspiration (resp., expiration) of the *parent* (i.e., 0th generation) airway. As in the single-compartment model, we assume that a pressure of $p_{\rm in}(t), t \geq 0$, is applied during inspiration.

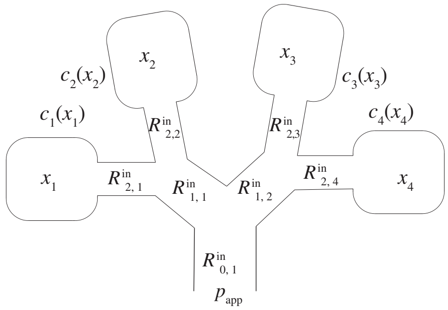

Fig. 4. Four-compartment lung model.

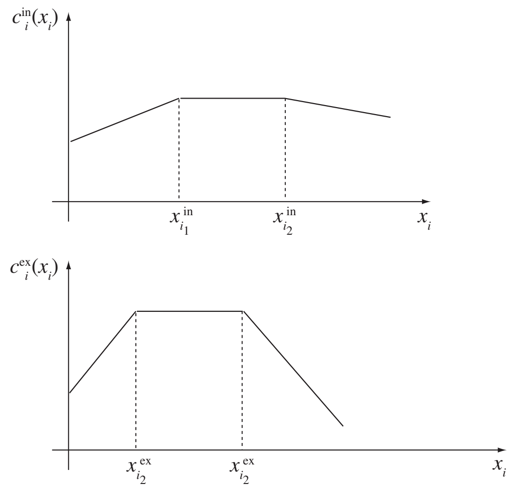

Fig. 5. Typical inspiration and expiration compliance functions as function of compartmental volumes.

Now, the state equations for inspiration are given by

$$R^{\rm in}_{n,i}\dot{x}_i(t) + \frac{1}{c^{\rm in}_i(x_i(t))}x_i(t) + \sum_{j=0}^{n-1} R^{\rm in}_{j,k_j} \times \sum_{l=(k_j-1)2^{n-j}+1}^{k_j 2^{n-j}} \dot{x}_l(t) = p_{\rm in}(t), \quad x_i(0) = x^{\rm in}_{i0}, \quad 0 \le t \le T_{\rm in}, \quad i = 1, 2, \ldots, 2^n \tag{45}$$

where $c^{\rm in}_i(x_i)$, $i = 1, 2, \ldots, 2^n$, are nonlinear functions of x_i, $i = 1, 2, \ldots, 2^n$, given by [40]

$$c^{\rm in}_i(x_i) \triangleq \begin{cases} a^{\rm in}_{i_1} + b^{\rm in}_{i_1}x_i, & \text{if } 0 \le x_i \le x^{\rm in}_{i_1}, \\ a^{\rm in}_{i_2}, & \text{if } x^{\rm in}_{i_1} \le x_i \le x^{\rm in}_{i_2}, \\ a^{\rm in}_{i_3} + b^{\rm in}_{i_3}x_i, & \text{if } x^{\rm in}_{i_2} \le x_i \le TV_i, \end{cases} \quad i = 1, \ldots, 2^n \tag{46}$$

where $a^{\rm in}_{i_j}$, $j = 1, 2, 3$, and $b^{\rm in}_{i_j}$, $j = 1, 3$, are unknown parameters with $b^{\rm in}_{i_1} > 0$ and $b^{\rm in}_{i_3} < 0$, $x^{\rm in}_{i_j}$, $j = 1, 2$, are unknown volume ranges wherein the compliance is constant, TV_i denotes tidal volume, and

$$k_j = \left\lfloor \frac{k_{j+1} - 1}{2} \right\rfloor + 1, \quad j = 0, \ldots, n-1, \quad k_n = i \tag{47}$$

where $\lfloor q \rfloor$ denotes the *floor function* which gives the largest integer less than or equal to the positive number q. Fig. 5 shows a typical piecewise linear compliance function for inspiration. A similar compliance representation holds for expiration, which is also shown in Fig. 5.

To further elucidate the inspiration state equation for a 2^n-compartment model, consider the four-compartment model shown in Fig. 4 corresponding to a two-generation lung model. Let x_i, $i = 1, 2, 3, 4$, denote the compartmental volumes. Now, the pressure $(1/c^{\rm in}_i(x_i(t))x_i(t))$ due to the compliance in the ith compartment will be equal to the difference between the external pressure applied and the resistance to air flow at every airway in the path leading from the pressure source to the ith compartment. In particular, for $i = 3$ (see Fig. 4)

$$\frac{1}{c^{\rm in}_3(x_3(t))}x_3(t) = p_{\rm in}(t) - R^{\rm in}_{0,1}[\dot{x}_1(t) + \dot{x}_2(t) + \dot{x}_3(t) + \dot{x}_4(t)] - R^{\rm in}_{1,2}[\dot{x}_3(t) + \dot{x}_4(t)] - R^{\rm in}_{2,3}\dot{x}_3(t)$$

or, equivalently

$$R^{\rm in}_{2,3}\dot{x}_3(t) + R^{\rm in}_{1,2}[\dot{x}_3(t) + \dot{x}_4(t)] + R^{\rm in}_{0,1}[\dot{x}_1(t) + \dot{x}_2(t) + \dot{x}_3(t) + \dot{x}_4(t)] + \frac{1}{c^{\rm in}_3(x_3(t))}x_3(t) = p_{\rm in}(t).$$

Next, we consider the state equation for the expiration process. As in the single-compartment model, we assume that the expiration process is passive and the external pressure applied is $p_{\rm ex}(t)$, $t \ge 0$. Following an identical procedure as in the inspiration case, we obtain the state equation for expiration as

$$R^{\rm ex}_{n,i}\dot{x}_i(t) + \sum_{j=0}^{n-1} R^{\rm ex}_{j,k_j} \sum_{l=(k_j-1)2^{n-j}+1}^{k_j 2^{n-j}} \dot{x}_l(t) + \frac{1}{c^{\rm ex}_i(x_i(t))}x_i(t) = p_{\rm ex}(t), \quad x_i(T_{\rm in}) = x^{\rm ex}_{i_0}, \quad T_{\rm in} \le t \le T_{\rm ex} + T_{\rm in}, \quad i = 1, 2, \ldots, 2^n \tag{48}$$

where

$$c^{\rm ex}_i(x_i) \triangleq \begin{cases} a^{\rm ex}_{i_1} + b^{\rm ex}_{i_1}x_i, & \text{if } 0 \le x_i \le x^{\rm ex}_{i_1}, \\ a^{\rm ex}_{i_2}, & \text{if } x^{\rm ex}_{i_1} \le x_i \le x^{\rm ex}_{i_2}, \\ a^{\rm ex}_{i_3} + b^{\rm ex}_{i_3}x_i, & \text{if } x^{\rm ex}_{i_2} \le x_i \le TV_i, \end{cases} \quad i = 1, \ldots, 2^n \tag{49}$$

$a^{\rm ex}_{i_j}$, $j = 1, 2, 3$, and $b^{\rm ex}_{i_j}$, $j = 1, 3$, are unknown parameters with $b^{\rm ex}_{i_1} > 0$ and $b^{\rm ex}_{i_3} < 0$, $x^{\rm ex}_{i_j}$, $j = 1, 2$, are unknown volume ranges wherein the compliance is constant, and k_j is given by (47).

V. Neuroadaptive Control for Pressure- and Work-Limited Mechanical Ventilation

In this section, we illustrate the efficacy of the neuroadaptive control framework of Section III on the nonlinear multi-compartmental lung model developed in Section IV. First, however, we rewrite the state equations (45) and (48) for inspiration and expiration, respectively, in the form of (2). Specifically, define the state vector $x \triangleq [x_1, x_2, \ldots, x_{2^n}]^{\mathrm{T}}$, where x_i denotes the lung volume of the ith compartment. Now, the state equation (45) for inspiration can be rewritten as

$$R_{\text{in}}\dot{x}(t) + C_{\text{in}}(x(t))x(t) = p_{\text{in}}(t)\mathbf{e}, \quad x(0) = x_0^{\text{in}}, \quad 0 \le t \le T_{\text{in}} \tag{50}$$

where $\mathbf{e} \triangleq [1, \ldots, 1]^{\mathrm{T}}$ denotes the ones vector of order 2^n, $C_{\text{in}}(x)$ is a diagonal matrix function given by

$$C_{\text{in}}(x) \triangleq \operatorname{diag}\left[\frac{1}{c_1^{\text{in}}(x_1)}, \cdots, \frac{1}{c_{2^n}^{\text{in}}(x_{2^n})}\right] \tag{51}$$

and

$$R_{\text{in}} \triangleq \sum_{j=0}^{n}\sum_{k=1}^{2^j} R_{j,k}^{\text{in}}\ Z_{j,k}\ Z_{j,k}^{\mathrm{T}} \tag{52}$$

where $Z_{j,k} \in \mathbb{R}^{2^n}$ is such that the l-th element of $Z_{j,k}$ is 1 for all $l = (k-1)2^{n-j}+1,\ (k-1)2^{n-j}+2, \ldots, k2^{n-j}, k = 1, \ldots, 2^j, j = 0, 1, \ldots, n$, and zero elsewhere.

Similarly, the state equation (48) for expiration can be rewritten as

$$R_{\text{ex}}\dot{x}(t) + C_{\text{ex}}(x(t))x(t) = p_{\text{ex}}(t)\mathbf{e}, \quad x(T_{\text{in}}) = x_0^{\text{ex}}, \quad T_{\text{in}} \le t \le T_{\text{ex}} + T_{\text{in}} \tag{53}$$

where

$$C_{\text{ex}}(x) \triangleq \operatorname{diag}\left[\frac{1}{c_1^{\text{ex}}(x_1)}, \cdots, \frac{1}{c_{2^n}^{\text{ex}}(x_{2^n})}\right] \tag{54}$$

and

$$R_{\text{ex}} \triangleq \sum_{j=0}^{n}\sum_{k=1}^{2^j} R_{j,k}^{\text{ex}}\ Z_{j,k}\ Z_{j,k}^{\mathrm{T}}. \tag{55}$$

Now, since, by Proposition 4.1 of [27], R_{in} and R_{ex} are invertible, it follows that (50) and (53) can be equivalently written as

$$\dot{x}(t) = A_{\text{in}}(x(t))x(t) + B_{\text{in}}p_{\text{in}}(t), \quad x(0) = x_0^{\text{in}}, \quad 0 \le t \le T_{\text{in}} \tag{56}$$

$$\dot{x}(t) = A_{\text{ex}}(x(t))x(t) + B_{\text{ex}}p_{\text{ex}}(t), \quad x(T_{\text{in}}) = x_0^{\text{ex}}, \quad T_{\text{in}} \le t \le T_{\text{ex}} + T_{\text{in}} \tag{57}$$

where $A_{\text{in}}(x) \triangleq -R_{\text{in}}^{-1}C_{\text{in}}(x)$, $B_{\text{in}} \triangleq R_{\text{in}}^{-1}\mathbf{e}$, $A_{\text{ex}}(x) \triangleq -R_{\text{ex}}^{-1}C_{\text{ex}}(x)$, and $B_{\text{ex}} \triangleq R_{\text{ex}}^{-1}\mathbf{e}$.

To account for a continuous transition of the lung resistance and compliance parameters between the inspiration and expiration phase, consider the bounded continuous periodic function $\theta(t) \in \mathbb{R}$, $t \ge 0$, given by

$$\theta(t) \triangleq \begin{cases} 1, & \text{if } 0 \le t \le T_{\text{in}} - \varepsilon_{\text{in}}, \\ \frac{1}{\varepsilon_{\text{in}}}(T_{\text{in}} - t), & \text{if } T_{\text{in}} - \varepsilon_{\text{in}} \le t \le T_{\text{in}} \\ 0, & \text{if } T_{\text{in}} \le t \le T_{\text{in}} + T_{\text{ex}} - \varepsilon_{\text{ex}} \\ \frac{1}{\varepsilon_{\text{ex}}}(t + \varepsilon_{\text{ex}} - T_{\text{in}} - T_{\text{ex}}), & \text{otherwise} \end{cases} \tag{58}$$

where $\varepsilon_{\text{in}} > 0$ and $\varepsilon_{\text{ex}} > 0$ are sufficiently small constants representing the transition times form inspiration to expiration and vice versa, respectively, and $\theta(t) = \theta(t + T_{\text{in}} + T_{\text{ex}})$ for all $t \ge 0$. It is important to note that small variations in the parameters ε_{in} and ε_{ex} result in imperceptible differences in the closed-loop system performance. Now, (56) and (57) can be written as

$$\begin{aligned}\dot{x}(t) = &\big[\theta(t)A_{\text{in}}(x(t)) + (1-\theta(t))A_{\text{ex}}(x(t))\big]x(t) \\ &+ [\theta(t)B_{\text{in}} + (1-\theta(t))B_{\text{ex}}]\,[h(u(t)) + P_{\text{ex}} \\ &+ P_{\text{musc}}(\mathbf{e}^{\mathrm{T}}x(t))\big],\ x(0) = x_{\text{in}}(0),\ t \ge 0\end{aligned} \tag{59}$$

where $u(t) \triangleq p_{\text{k}}(t)$, $\text{k} \in \{\text{in}, \text{ex}\}$, $t \ge 0$, $z(t) \triangleq \int_{t-\tau_{\text{m}}}^{t}\mathbf{e}^{\mathrm{T}}x(s)\mathrm{d}s$, $\tau_{\text{m}} > 0$, $t \ge 0$, $h(u(t))$, $t \ge 0$, is a saturation constraint on the applied airway pressure given by

$$h(u) \triangleq \begin{cases} 0, & \text{if } u \le 0, \\ P_{\max}, & \text{if } u \ge P_{\max}, \\ u, & \text{otherwise.} \end{cases} \tag{60}$$

$P_{\text{ex}} \in \mathbb{R}^{2^n}$ denotes the end-expiratory pressure due to air remaining in the lung after the completion of each breath [40], $P_{\max}$ denotes the peak pressure of the ventilator, and $P_{\text{musc}}(\mathbf{e}^{\mathrm{T}}x(t), z(t))$, $t \ge 0$, introduced in (59) represents a nonnegative pressure term due to the lung muscle activity of a patient and accounts for the effect of spontaneous breathing of a patient in the lung model. Here, we assume that $P_{\text{musc}}(\mathbf{e}^{\mathrm{T}}x(t), z(t))$, $t \ge 0$, is a nonlinear function given by

$$P_{\text{musc}}(\mathbf{e}^{\mathrm{T}}x(t), z(t)) = e^{-\alpha_{\text{p}}t}\kappa(t)W_{\text{m}}^{\mathrm{T}}\sigma_{\text{m}}(\mathbf{e}^{\mathrm{T}}x(t), z(t)), \quad t \ge 0 \tag{61}$$

where $\alpha_{\text{p}} \ge 0$, $\kappa : \mathbb{R} \to \mathbb{R}$ is a given bounded function, $W_{\text{m}} \in \mathbb{R}^{l_m \times 2^n} \ge\ge 0$ is an *unknown* matrix, and $\sigma_{\text{m}}(\mathbf{e}^{\mathrm{T}}x, z) : \mathbb{R}\times\mathbb{R} \to \overline{\mathbb{R}}_+^{l_m}$ is a known function of the instantaneous system volume as well as past system volume over a moving time window. The scaling factor $e^{-\alpha_{\text{p}}t}\kappa(t)$ in (61) is introduced to account for the effect of the anesthetic on the spontaneous breathing of the patient. Specifically, if α_{p} is large, indicating a heavily sedated patient, then the lung muscle activity of the patient is negligible, whereas if α_{p} is small, indicating a moderately sedated or agitated patient, then the lung muscle activity of the patient is accounted for by (61).

Note that since, by Proposition 4.1 of [27], $-R_{\text{in}}^{-1}$ and $-R_{\text{ex}}^{-1}$ are essentially nonnegative, $C_{\text{in}}(x)$ and $C_{\text{ex}}(x)$ are diagonal, and $\theta(t) \ge 0$, $t \ge 0$, it follows that $A_{\text{in}}(x)$ and $A_{\text{ex}}(x)$ in (59) are essentially nonnegative. Hence, since $h(u(t)) \ge\ge 0$, $t \ge 0$, $P_{\text{musc}}(\mathbf{e}^{\mathrm{T}}x(t), z(t)) \ge\ge 0$, $t \ge 0$, and $P_{\text{ex}} \ge\ge 0$, it follows from Proposition 1 that $x(t) \ge\ge 0$, $t \ge 0$, for all $x_{\text{in}}(0) \in \overline{\mathbb{R}}_+^{2^n}$.

Next, we rewrite (59) in the form of (2) and (3) as

$$\dot{x}(t) = A_0x(t) + B_0h(u(t)) + f(x(t), h(u(t)), \theta(t)), \quad x(0) = x_{\text{in}}(0), \quad t \ge 0 \tag{62}$$

$$y(t) = Cx(t) \tag{63}$$

where $A_0 = -R_{\text{av}}^{-1}C_{\text{av}}$, $B_0 = R_{\text{av}}^{-1}\mathbf{e}$, and $C = \mathbf{e}^{\mathrm{T}}$, and R_{av} and C_{av} are nominal parameter matrices given by

$$R_{\text{av}} \triangleq \sum_{j=0}^{n}\sum_{k=1}^{2^j} R_{j,k}^{\text{av}}\ Z_{j,k}\ Z_{j,k}^{\mathrm{T}}, \quad C_{\text{av}} \triangleq \operatorname{diag}\left[\frac{1}{c_1^{\text{av}}}, \cdots, \frac{1}{c_{2^n}^{\text{av}}}\right]$$

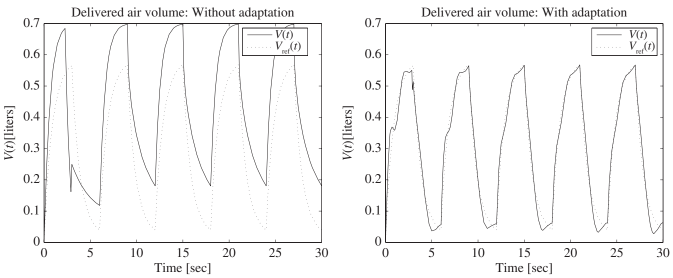

Fig. 6. Delivered air volume $V(t) = \mathbf{e}^{\mathrm{T}}x(t)$ versus time with pressure-limited input $h(u(t))$.

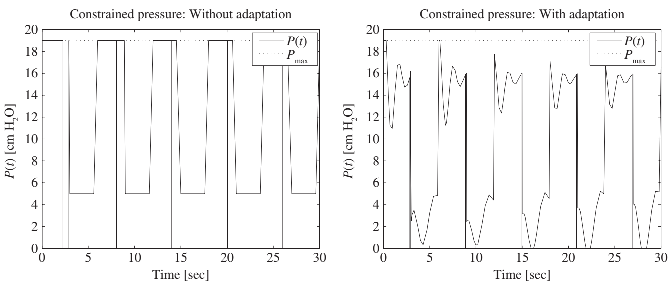

Fig. 7. Constrained pressure $P(t) = h(u(t))$ versus time.

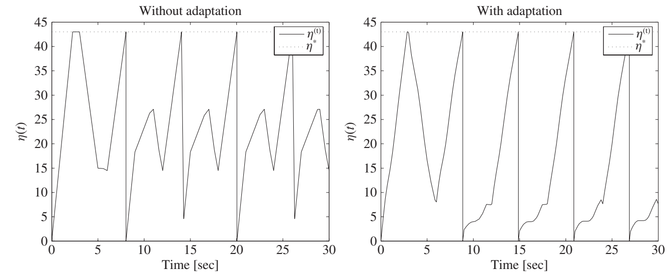

Fig. 8. $\eta(t)$ versus time.

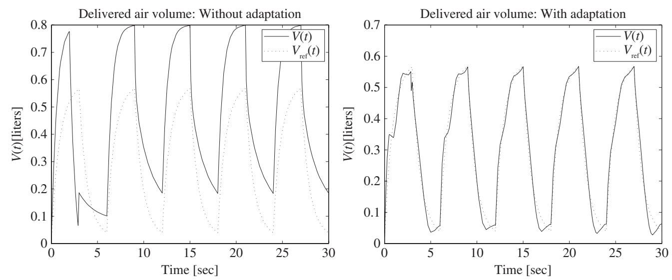

Fig. 9. Delivered air volume $V(t) = \mathbf{e}^{\mathrm{T}}x(t)$ versus time with unconstrained pressure input $u(t)$.

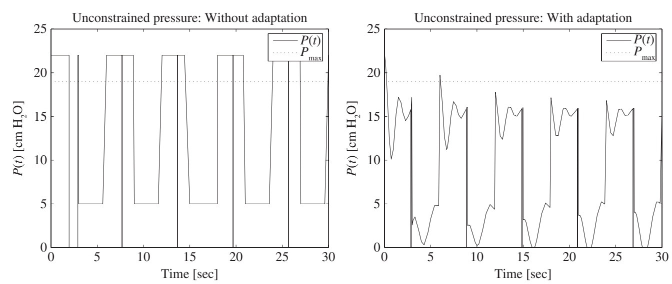

Fig. 10. Unconstrained pressure $P(t) = u(t)$ versus time.

where $R^{\mathrm{av}}_{j,i}$, $i = 1, 2, \ldots, 2^j$, $j = 0, \ldots, n$, denote the nominal resistance (to air flow) of the ith airway in the jth generation, and c^{av}_i, $i = 1, 2, \ldots, 2^n$, denote the nominal compliance of each compartment. Now, the nonlinear unknown function $f(x, h(u), \theta)$ capturing resistance and compliance uncertainty in (62) during the inspiration and expiration phases is given by

$$\begin{aligned} f(x, h(u), \theta) = {} & [\theta(A_{\mathrm{in}}(x) - A_0) + (1-\theta)(A_{\mathrm{ex}}(x) - A_0)]x \\ & + [\theta(B_{\mathrm{in}} - B_0) + (1-\theta)(B_{\mathrm{ex}} - B_0)] \\ & \times [h(u) + P_{\mathrm{musc}}(\mathbf{e}^{\mathrm{T}}x) + P_{\mathrm{ex}}]. \qquad (64) \end{aligned}$$

Finally, to account for work limitation constraints by the mechanical ventilator over an inspiration-expiration cycle, we assume that the constraint (7) holds and is given by $\eta(t) \triangleq \int_{t-\tau_l}^{t} h(u(s))\mathrm{d}s \le \eta^*$, $t \ge 0$, $\tau_l > 0$, where $\eta^* > 0$.

Our goal here is to design a neuroadaptive controller satisfying the aforementioned input constraints while guaranteeing output tracking of a clinically plausible reference model in the face of physiological parameter uncertainty. For the system given by (62) and (63), which is a special case of (2) and (3), we consider an output tracking problem with a reference model of the form given by (5) and (6), and design a neuroadaptive controller using Theorem 1.

For our simulation, we consider a two-compartment lung model and use the values for lung resistance and compliance found in [40]. In particular, we set $c^{\mathrm{av}}_1 = 0.022\,\ell/\mathrm{cm}\ H_2O$, $c^{\mathrm{av}}_2 = 0.03\,\ell/\mathrm{cm}\ H_2O$, $a^{\mathrm{in}}_{i_1} = 0.018\,\ell/\mathrm{cm}\ H_2O$, $b^{\mathrm{in}}_{i_1} = 0.0233$, $a^{\mathrm{in}}_{i_2} = 0.025\,\ell/\mathrm{cm}\ H_2O$, $a^{\mathrm{in}}_{i_3} = 0.2532\,\ell/\mathrm{cm}\ H_2O$, $b^{\mathrm{in}}_{i_3} = -0.0067$, $x^{\mathrm{in}}_{i_1} = 0.3\,\ell$, $x^{\mathrm{in}}_{i_2} = 0.48\,\ell$, $x^{\mathrm{in}}_{i_3} = 0.63\,\ell$, $i = 1, 2$, $a^{\mathrm{ex}}_{i_1} = 0.02\,\ell/\mathrm{cm}\ H_2O$, $b^{\mathrm{ex}}_{i_1} = 0.078$, $a^{\mathrm{ex}}_{i_2} = 0.038\,\ell/\mathrm{cm}\ H_2O$, $a^{\mathrm{ex}}_{i_3} = 0.1025\,\ell/\mathrm{cm}\ H_2O$, $b^{\mathrm{ex}}_{i_3} = -0.15$, $x^{\mathrm{ex}}_{i_1} = 0.23\,\ell$, $x^{\mathrm{ex}}_{i_2} = 0.43\,\ell$, $x^{\mathrm{ex}}_{i_3} = 0.63\,\ell$, $i = 1, 2$, $R^{\mathrm{av}}_{0,1} = 6.29$ cm H_2O/ℓ/sec, $R^{\mathrm{av}}_{1,1} = 30.67$ cm H_2O/ℓ/sec, $R^{\mathrm{av}}_{1,2} = 13$ cm H_2O/ℓ/sec, $R^{\mathrm{in}}_{0,1} = 6$ cm H_2O/ℓ/sec, $R^{\mathrm{in}}_{1,1} = 25$ cm H_2O/ℓ/sec, $R^{\mathrm{in}}_{1,2} = 10$ cm H_2O/ℓ/sec, $R^{\mathrm{ex}}_{0,1} = 6$ cm H_2O/ℓ/sec, $R^{\mathrm{ex}}_{1,1} = 40$ cm H_2O/ℓ/sec, $R^{\mathrm{ex}}_{1,2} = 20$ cm H_2O/ℓ/sec, $T_{\mathrm{in}} = 5$ sec, $T_{\mathrm{ex}} = 10$ sec, $\varepsilon_{\mathrm{in}} = \varepsilon_{\mathrm{ex}} = 0.001$ sec, $P_{\mathrm{ex}}(t) = \theta(t)P^1_{\mathrm{ex}} + (1-\theta(t))P^2_{\mathrm{ex}}$, $P^1_{\mathrm{ex}} = [-0.1105, -0.3113]^{\mathrm{T}}$ cm H_2O, $P^2_{\mathrm{ex}} = [-0.0894, -0.1964]^{\mathrm{T}}$ cm H_2O, $W_{\mathrm{m}} = [0.01, 0.03, 0.23, 0; 0.02, 0.01, 0, 0.17]^{\mathrm{T}}$, and $\sigma_{\mathrm{m}}(y, z) = [1/(1 + e^{-0.2y}), 1/(1 + e^{-0.3y})1/(1 + e^{-0.3z}), 1/(1 + e^{-0.5z})]^{\mathrm{T}}$.

TABLE I

MAE, MAXIMUM VOLUME UNDERSHOOT, AND MAXIMUM VOLUME OVERSHOOT

	Without adaptation	With adaptation
MAE (%)	53.98	0.94
Max. overshoot (%)	364.46	92.43
Max. undershoot (%)	88.33	64.96

For our first simulation, we set $A_{\mathrm{ref}} = A_0$, $B_{\mathrm{ref}} = 0.6B$, $r(t) = 17\theta(t) + 5$ cm H_2O, $K_{\mathrm{r}} = 0.6$, $\sigma(\zeta(t), h(u(t))) = [1/(1 + e^{-ay(t)}), 1/(1 + e^{-ay(t-d)}), 1/(1 + e^{-aP(t)}), \theta(t), \sigma^{\mathrm{T}}_{\mathrm{m}}(y(t), 0)]^{\mathrm{T}}$, $t \ge 0$, $a = 0.02$, $x_0 = x_{\mathrm{ref}0} = [0, 0]^{\mathrm{T}}$, $\hat{W}_0 = 0_{8\times 2}$, $\Gamma_W = 100 I_8$, $W_{\mathrm{m}} = [0.01, 0.03, 0, 0;$

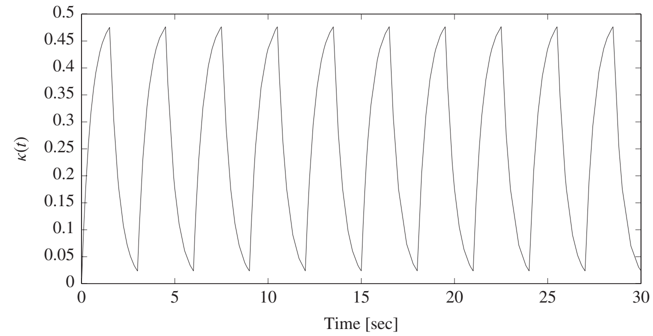

Fig. 11. $\kappa(t)$ versus time.

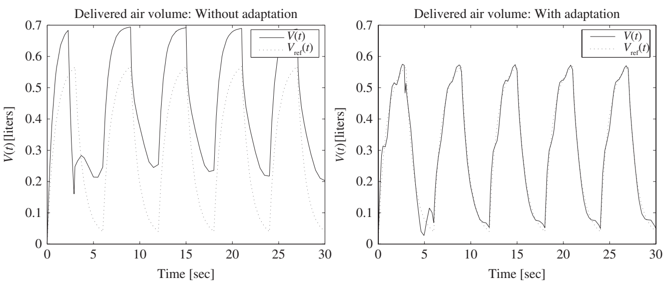

Fig. 12. Delivered air volume $V(t) = \mathbf{e}^{\mathrm{T}} x(t)$ versus time with pressure-limited input $h(u(t))$.

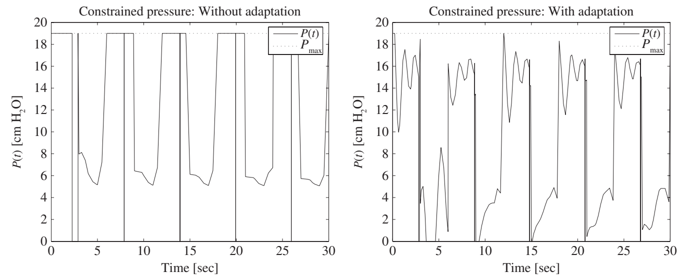

Fig. 13. Constrained pressure $P(t) = h(u(t))$ versus time.

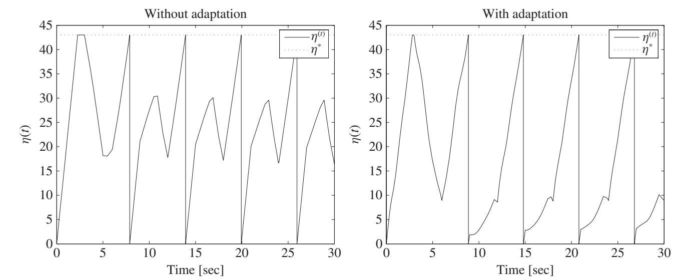

Fig. 14. $\eta(t)$ versus time.

0.02, 0.01, 0, 0$]^{\mathrm{T}}$, peak pressure limit $P_{\max} = 19$ cm H_2O, and $\eta^* = 43$ sec·cm H_2O. From the structure of W_{m} and $\sigma_{\mathrm{m}}(y, 0)$ it follows that lung muscle activity of the patient is not a function of the past system volume. In addition, we set $\alpha_{\mathrm{p}} = 0$ and $\kappa(t) \equiv 1$. Figs. 6–8 show the delivered air volume $V(t) = \mathbf{e}^{\mathrm{T}} x(t)$ versus time, the constrained pressure $P(t) = h(u(t))$ versus time, and the integrated constrained pressure over the time interval $\tau_l = 5$ s with and without adaptation for the pressure-limited input $h(u(t))$, $t \geq 0$. Figs. 9 and 10 show the delivered air volume versus time and the unconstrained pressure input $u(t)$, $t \geq 0$, versus time with and without adaptation. Here, "with adaptation" refers to the control signal (16) with the adaptive signal $\psi_{\mathrm{ad}}(t)$, $t \geq 0$, given by (20), and "without adaptation" refers to the control signal (16) with $\psi_{\mathrm{ad}}(t) \equiv 0$. In addition, Table I summarizes performance measures of the control algorithm with and without adaptation for mean absolute error (MAE) (defined as measured delivered volume minus the target volume, normalized to the target), maximum volume overshoot, and maximum volume undershoot. It can be seen from Table I that adaptation provides significantly better tracking performance of the reference model.

As can be seen from Fig. 6, the delivered air volume significantly exceeds the desired values in the absence of adaptation, whereas satisfactory tracking of the desired air volume is achieved with adaptation. As discussed in the introduction, failure to adequately regulate the mode and parameters of ventilatory support can result in failure to oxygenate, failure to achieve adequate lung expansion or overexpansion of the lung resulting in lung tissue rupture. These problems oftentimes occur when open-loop volume control or pressure control is employed or when averaged respiratory data is used to choose the parameters for a closed-loop ventilation control algorithm. In contrast, the proposed neuroadaptive control algorithm avoids reliance on average respiratory data and achieves system performance without excessive reliance on system model parameters.

TABLE II

MAE, MAXIMUM VOLUME UNDERSHOOT, AND MAXIMUM VOLUME OVERSHOOT

	Without Adaptation	With Adaptation
MAE (%)	29.86	1.83
Max Overshoot (%)	539.52	129.21
Max Undershoot (%)	71.47	66.57

Finally, to account for the lung muscle activity being a function of the instantaneous system volume as well as the past system volume, we set $\tau_{\mathrm{m}} = 3$ s and $\sigma(\zeta(t), h(u(t))) = [1/(1 + e^{-ay(t)}), 1/(1 + e^{-ay(t-d)}), 1/(1 + e^{-aP(t)}), \theta(t), \sigma_{\mathrm{m}}^{\mathrm{T}}(y(t), z(t))]^{\mathrm{T}}$, $t \geq 0$. In addition, to account for the effect of the anesthetic agent on spontaneous breathing, we set $\alpha_{\mathrm{p}} = 0.03$ and $\kappa(t)$ to be a saw-type function generated by filtering a pulse function of period 3 s and amplitude 1 through a first-order filter with a pole at -2 (see Fig. 11). Figs. 12–14 show the effect of the integral term $z(t)$, $t \geq 0$, in the muscle activity model. As can be seen from Fig. 12, in the absence of adaptation the delivered volume dynamics significantly differs from the dynamics shown in Fig. 6. However, as can be seen from Fig. 12, the neuroadaptive controller captures the effect of the integral term $z(t)$, $t \geq 0$, and provides satisfactory tracking of the reference model. Table II gives analogous performance measures to Table I for the case where lung muscle activity is accounted for in the simulations.

VI. CONCLUSION

Acute respiratory failure due to infection, trauma, and major surgery is one of the most common problems encountered in intensive care units and mechanical ventilation is the mainstay of supportive therapy for such patients. In particular, mechanical ventilation of a patient with respiratory failure is a critical life-saving procedure performed in the intensive care unit. Failure to adequately regulate the mode and parameters of ventilatory support can result in failure to oxygenate, failure to achieve adequate lung expansion, or overexpansion of the lung resulting in lung tissue rupture. In this paper, we developed a neuroadaptive control algorithm for mechanical ventilation to control lung volume and minute ventilation. The adaptive controller accounts for input pressure constraints as well as work of breathing constraints in the face of lung resistance and compliance model uncertainty.

References

[1] M. J. Tobin, *Principles and Practice of Mechanical Ventilation*. New York: McGraw-Hill, 1994.

[2] S. P. Pilbeam and J. M. Cairo, *Mechanical Ventilation, Physiological and Clinical Applications*, 4th ed. St. Louis, MO: Mosby, 1987.

[3] L. Martin, *Pulmonary Physiology in Clinical Practice*. St. Louis, MO: Mosby, 1987.

[4] J. B. West, *Respiratory Physiology*. Baltimore, MD: Williams & Wilkins, 2008.

[5] M. C. Khoo, R. E. Kronauer, K. P. Strohl, and A. S. Slutsky, "Factors inducing periodic breathing in humans: A general model," *J. Appl. Physiol.*, vol. 53, no. 3, pp. 644–659, Sep. 1982.

[6] J. J. Batzel and H. T. Trana, "Modeling instability in the control system for human respiration: Applications to infant non-REM sleep," *Appl. Math. Comput.*, vol. 110, no. 1, pp. 1–51, Apr. 2000.

[7] M. Younes, "Proportional assist ventilation," in *Principles and Practice of Mechanical Ventilation*, M. J. Tobin, Ed. New York: McGraw-Hill, 1994, pp. 349–369.

[8] M. Younes, A. Puddy, D. Roberts, R. B. Light, A. Quesada, K. Taylor, L. Oppenheimer, and H. Cramp, "Proportional assist ventilation: Results of an initial clinical trial," *Amer. Rev. Resp. Des.*, vol. 145, no. 1, pp. 121–129, 1992.

[9] T. P. Laubscher, W. Heinrichs, and N. Weiler, "An adaptive lung ventilation controller," *IEEE Trans. Biomed. Eng.*, vol. 41, no. 1, pp. 51–59, Jan. 1994.

[10] M. Dojat, L. Brochard, F. Lemaire, and A. Harf, "A knowledge-based system for assisted ventilation of patients in intensive care units," *Int. J. Clin. Monitor. Comput.*, vol. 9, no. 4, pp. 239–250, 1992.

[11] C. Sinderby, P. Navalesi, J. Beck, Y. Skrobik, N. Comtois, S. Friberg, S. B. Gottfried, and L. Lindström, "Neural control of mechanical ventilation in respiratory failure," *Natural Med.*, vol. 5, no. 12, pp. 1433–1436, 1999.

[12] M. Younes, "Proportional assist ventilation, a new approach to ventilatory support: Theory," *Amer. Rev. Resp. Des.*, vol. 145, no. 1, pp. 114–120, 1992.

[13] F. T. Tehrani, "Automatic control of an artificial respirator," in *Proc. Int. Conf. IEEE Eng. Med. Biol. Soc.*, vol. 13. Nov. 1991, pp. 1738–1739.

[14] L. Bouadma, F. Lellouche, B. Cabello, S. Taille, J. Mancebo, M. Dojat, and L. Brochard, "Computer-driven management of prolonged mechanical ventilation and weaning: A pilot study," *Intens. Care Med.*, vol. 31, no. 10, pp. 1446–1450, 2005.

[15] F. Lellouche, J. Mancebo, P. Jolliet, J. Roeseler, F. Shortgen, M. Dojat, B. Cabello, L. Bouadma, P. Rodriguez, S. Maggiore, M. Reynaert, S. Mersmann, and L. Brochard, "A multicenter randomized trial of computer-driven protocolized weaning from mechanical ventilation," *Amer. J. Resp. Crit. Care Med.*, vol. 174, pp. 894–900, Jul. 2006.

[16] A. Huszczuk, "A respiratory pump controlled by phrenic nerve activity," *J. Physiol.*, vol. 210, no. 2, pp. 183–184, 1970.

[17] J. Barwing, M. Ambold, N. Linden, M. Quintel, and O. Moerer, "Evaluation of the catheter positioning for neurally adjusted ventilatory assist," *Intens. Care Med.*, vol. 35, no. 10, pp. 1809–1814, 2009.

[18] O. Moerer, J. Beck, L. Brander, R. Costa, M. Quintel, A. S. Slutsky, F. Brunet, and C. Sinderby, "Subject–ventilator synchrony during neural versus pneumatically triggered non-invasive helmet ventilation," *Intens. Care Med.*, vol. 34, no. 9, pp. 1615–1623, 2008.

[19] J. Beck, M. Reilly, G. Grasselli, L. Mirabella, A. S. Slutsky, M. S. Dunn, and C. Sinderby, "Patient-ventilator interaction during neutrally adjusted ventilatory assist in low birth weight infants," *Pedia. Res.*, vol. 65, no. 6, pp. 663–668, Jun. 2009.

[20] W. M. Haddad, T. Hayakawa, and J. M. Bailey, "Adaptive control for nonnegative and compartmental dynamical systems with applications to general anesthesia," *Int. J. Adapt. Control Signal Process.*, vol. 17, no. 3, pp. 209–235, Apr. 2003.

[21] T. Hayakawa, W. M. Haddad, J. M. Bailey, and N. Hovakimyan, "Passivity-based neural network adaptive output feedback control for nonlinear nonnegative dynamical systems," *IEEE Trans. Neural Netw.*, vol. 16, no. 2, pp. 387–398, Mar. 2005.

[22] J. M. Bailey and W. M. Haddad, "Paradigms, benefits, and challenges - Drug-dosing control in clinical pharmacology," *IEEE Control Syst. Mag.*, vol. 25, no. 2, pp. 35–51, Apr. 2005.

[23] W. M. Haddad, T. Hayakawa, and J. M. Bailey, "Adaptive control for nonlinear compartmental dynamical systems with applications to clinical pharmacology," *Syst. Control Lett.*, vol. 55, no. 1, pp. 62–70, Jan. 2006.

[24] W. M. Haddad, J. M. Bailey, T. Hayakawa, and N. Hovakimyan, "Neural network adaptive output feedback control for intensive care unit sedation and intraoperative anesthesia," *IEEE Trans. Neural Netw.*, vol. 18, no. 4, pp. 1049–1066, Jul. 2007.

[25] Q. Hui, W. M. Haddad, V. Chellaboina, and T. Hayakawa, "Adaptive control of mammillary drug delivery systems with actuator amplitude constraints and system time delays," *Eur. J. Control*, vol. 11, no. 6, pp. 586–600, 2005.

[26] M. Chen, S. S. Ge, and B. How, "Robust adaptive neural network control for a class of uncertain MIMO nonlinear systems with input nonlinearities," *IEEE Trans. Neural Netw.*, vol. 21, no. 5, pp. 796–812, May 2010.

[27] V. Chellaboina, W. M. Haddad, J. M. Bailey, and H. Li, "Limit cycle stability analysis of a multi-compartment model for a pressure-limited respirator and lung mechanics system," in *Proc. Amer. Control Conf.*, 2007, pp. 2024–2029.

[28] W. M. Haddad and V. Chellaboina, "Stability and dissipativity theory for nonnegative dynamical systems: A unified analysis framework for biological and physiological systems," *Nonlinear Anal.: Real World Appl.*, vol. 6, no. 1, pp. 35–65, Feb. 2005.

[29] W. M. Haddad, V. Chellaboina, and Q. Hui, *Nonnegative and Compartmental Dynamical Systems*. Princeton, NJ: Princeton Univ. Press, 2010.

[30] S. S. Ge and C. Wang, "Adaptive NN control of uncertain nonlinear pure-feedback systems," *Automatica*, vol. 38, no. 4, pp. 671–682, Apr. 2002.

[31] W. Zhang and S. S. Ge, "A global implicit function theorem without initial point and its applications to control of non-affine systems of high dimensions," *J. Math. Anal. Appl.*, vol. 313, no. 1, pp. 251–261, Jan. 2006.

[32] H. L. Royden, *Real Analysis*. New York: Macmillan, 1988.

[33] F. L. Lewis, S. Jagannathan, and A. Yesildirak, *Neural Network Control of Robot Manipulators and Nonlinear Systems*. London, U.K.: Taylor & Francis, 1999.

[34] E. Lavretsky, N. Hovakimyan, and A. J. Calise, "Upper bounds for approximation of continuous-time dynamics using delayed outputs and feedforward neural networks," *IEEE Trans. Autom. Control*, vol. 48, no. 9, pp. 1606–1610, Sep. 2003.

[35] G. Tao, *Adaptive Control Design and Analysis*. New York: Wiley, 2003.

[36] W. M. Haddad and V. Chellaboina, *Nonlinear Dynamical Systems and Control: A Lyapunov-Based Approach*. Princeton, NJ: Princeton Univ. Press, 2008.

[37] W. M. Haddad, K. Y. Volyanskyy, J. M. Bailey, and J. J. Im, "Neuroadaptive output feedback control for automated anesthesia with noisy EEG measurements," *IEEE Trans. Control Syst. Technol.*, vol. 19, no. 2, pp. 311–326, Mar. 2011.

[38] N. Hovakimyan, F. Nardi, A. Calise, and N. Kim, "Adaptive output feedback control of uncertain nonlinear systems using single-hidden-layer neural networks," *IEEE Trans. Neural Netw.*, vol. 13, no. 6, pp. 1420–1431, Nov. 2002.

[39] E. R. Weibel, *Morphometry of the Human Lung*. New York: Academic, 1963.

[40] P. S. Crooke, J. J. Marini, and J. R. Hotchkiss, "Modeling recruitment maneuvers with a variable compliance model for pressure controlled ventilation," *J. Theor. Med.*, vol. 4, no. 3, pp. 197–207, 2002.

Kostyantyn Y. Volyanskyy (S'07–M'10) received the B.S., M.S., and Ph.D. degrees in applied mathematics from the National Taras Shevchenko University of Kyiv, Kiev, Ukraine, in 1998, 1999, and 2003, respectively, with a specialization in modeling and control of complex dynamical systems. He received another Ph.D. degree in aerospace engineering from the Georgia Institute of Technology, Atlanta, in 2010.

He is currently a Post-Doctoral Fellow at the Georgia Institute of Technology. His current research interests include nonlinear adaptive control and estimation, neural networks and intelligent control, nonlinear analysis and control for biological and physiological systems, and active control for clinical pharmacology.

Wassim M. Haddad (S'87–M'87–SM'01–F'09) received the B.S., M.S., and Ph.D. degrees in mechanical engineering from the Florida Institute of Technology, Melbourne, in 1983, 1984, and 1987, respectively, with a specialization in dynamical systems and control.

He served as a Consultant for the Structural Controls Group of the Government Aerospace Systems Division, Harris Corporation, Melbourne, from 1987 to 1994. In 1988, he joined the faculty of the Mechanical and Aerospace Engineering Department, Florida Institute of Technology, where he founded and developed the systems and control option within the graduate program. Since 1994, he has been a member of the Faculty in the School of Aerospace Engineering at the Georgia Institute of Technology, Atlanta, where he holds the rank of Professor and Chair of the Flight Dynamics and Control discipline. His research contributions in linear and nonlinear dynamical systems and control are documented in over 520 archival journal and conference publications. He is a co-author of the books *Hierarchical Nonlinear Switching Control Design with Applications to Propulsion Systems* (Springer-Verlag, 2000), *Thermodynamics: A Dynamical Systems Approach* (Princeton University Press, 2005), *Impulsive and Hybrid Dynamical Systems: Stability, Dissipativity, and Control* (Princeton University Press, 2006), *Nonlinear Dynamical Systems and Control: A Lyapunaov-Based Approach* (Princeton University Press, 2008), *Nonnegative and Compartmental Dynamical Systems* (Princeton University Press, 2010), and *Stability and Control of Large-Scale Systems* (Princeton University Press, 2011). His current research interests include nonlinear robust and adaptive control, nonlinear dynamical system theory, large-scale systems, hierarchical nonlinear switching control, analysis and control of nonlinear impulsive and hybrid systems, adaptive and neuroadaptive control, system thermodynamics, thermodynamic modeling of mechanical and aerospace systems, network systems, expert systems, nonlinear analysis and control for biological and physiological systems, and active control for clinical pharmacology. His secondary interests include the history of science and mathematics, as well as western philosophy.

Prof. Haddad is a National Science Foundation Presidential Faculty Fellow and a member of the Academy of Nonlinear Sciences.

James M. Bailey received the B.S. degree from Davidson College, Davidson, NC, in 1969, the Ph.D. degree in chemistry (physical) from the University of North Carolina, Chapel Hill, in 1973, and the M.D. degree from Southern Illinois University School of Medicine, Springfield, in 1982.

He was a Helen Hay Whitney Fellow at the California Institute of Technology, Pasadena, from 1973 to 1975, and an Assistant Professor of chemistry and biochemistry at Southern Illinois University from 1975 to 1979. After receiving the M.D. degree, he completed a residency in anesthesiology and then a fellowship in cardiac anesthesiology at the Emory University School of Medicine Affiliated Hospitals, Atlanta, GA. From 1986 to 2002, he was an Assistant Professor of anesthesiology and then Associate Professor of anesthesiology at the Emory University School of Medicine Affiliated Hospitals, where he also served as a Director of Critical Care Service. In September 2002, he moved his clinical practice to Northeast Georgia Medical Center, Gainesville, as a Director of Cardiac Anesthesia and Consultant in critical care medicine. He has served as Chief Medical Officer of Northeast Georgia Health Systems, Gainesville, since 2008. He is board certified in anesthesiology, critical care medicine, and transesophageal echocardiography. He is the author or co-author of over 100 journal articles, conference publications, and book chapters. His current research interests include pharmacokinetic and pharmacodynamic modeling of anesthetic and vasoactive drugs and applications of dynamical system theory in medicine.